



This is a non-peer-reviewed preprint submitted to EarthArXiv.

An Event-Based Framework for Estimating Annual Methane Emissions and Managing Emissions Data from Upstream Oil and Gas Facilities

Mozhou Gao^{1,4}, Zahra Ashena^{1,3}, Steve H.L. Liang^{1,3}, Sina Kiaei^{1,3}, and Sara Saeedi^{1,2}

¹GeoSensorWeb Lab, Department of Geomatics Engineering, Schulich School of Engineering, University of Calgary, 2500 University Dr. NW, Calgary, AB, Canada

²Department of Electrical and Software Engineering, Schulich School of Engineering, University of Calgary, 2500 University Dr. NW, Calgary, AB, Canada

³SensorUp Inc., Calgary, AB, Canada

⁴Kuruktag Emissions Ltd., Coquitlam, BC, Canada

Email: mozhou.gao@ucalgary.ca

Abstract

Accurate reporting of annual site-level methane emissions is increasingly required under emerging regulatory and voluntary frameworks in the oil and gas (O&G) sector. In this study, we present an event-based framework for estimating annual methane emissions from upstream O&G facilities. The framework applies the Emission Event Data Model (EEDM) to spatiotemporally aggregate multi-scale emissions data into discrete events using the concept of Allen's interval algebra and spatial proximity. Following the creation of events, emissions are categorized into three groups: resolved (with a known emission rate and duration), partially resolved (with a known emission rate but an unknown duration), and unresolved (with an unknown emission rate and duration) to facilitate various management and emissions estimation approaches. To estimate emissions and its associated uncertainties using events, we developed three Monte Carlo-based approaches, which are (1) estimating durations for partially resolved events using null detections and leak generation and natural repair processes; (2) estimating emissions from unresolved events based on the minimum detection limit of deployed technologies; and (3) estimating emissions from unresolved events using probabilistic occurrence and best-fit rate and duration distributions. This framework enables emissions to be reported and verified at a uniform scale rather than at the individual observation scale. To demonstrate the estimation of emissions using this framework, we created two case studies. In both studies, we performed emissions estimation using emission observations synthesized from real emissions data from an upstream O&G site. The proposed framework and methodologies can be implemented in voluntary initiatives such as Veritas 2.0 and the Oil & Gas Methane Partnership 2.0 and the event data model can be applied as a data management framework for the Measurement, Monitoring, Reporting, and Verification (MMRV) framework.

Keywords: Oil and Gas Methane, Greenhouse Gases, Emissions Data model, Event-based approaches, Estimating Unmeasured Emissions, Annual Emissions Estimation, MMRV Framework

Highlights:

1. This study addresses the fundamental challenges of data integration in estimating annual methane emissions.
2. This study presents the first event-based framework to assimilate multi-scale methane emissions measurements and oil and gas operational data.
3. This study focuses not only on the rate of emissions but also on the duration and uncertainties in emissions estimation.
4. This study presents two new Monte Carlo–based approaches to estimating unmeasured methane emissions.
5. The presented data model and methodology will help oil and gas operators better understand and track their emissions mitigation progress.

1. Introduction

Reducing methane (CH₄) emissions from the oil and gas (O&G) sector is internationally recognized as one of the most cost-effective strategies for mitigating global warming.¹ This effort gained significant momentum following the launch of the Global Methane Pledge at the 2021 United Nations Climate Change Conference (COP26), where 159 countries pledged to reduce methane emissions by 30% from 2020 levels by 2030.² Since then, participants worldwide have made substantial efforts to develop innovative measurement technologies and emissions estimation frameworks. Regulators, such as the U.S. Environmental Protection Agency (EPA) and the European Commission (EC), have further tightened regulatory requirements in recent years to help achieve these reduction targets.^{3,4}

The Measuring, Monitoring, Reporting, and Verification (MMRV; also with a variant that emphasizes the importance of quantification, known as the Measuring, Quantification, Reporting and Verification framework, [e.g., ref 5]) is in the process of implementation and widely recognized as one of the most effective and transparent frameworks for tracking annual emissions in the oil and gas.^{6,7}

Measuring and quantification refer to the deployment of measurement technologies to directly measure and quantify emissions, including using remote sensing systems and close-range instruments. For emission sources that have already been identified, monitoring is conducted either

through continuous monitoring systems or revisits using snapshot technologies to assess the emission source and its activity. Reporting refers to the standardized documentation and disclosure of emissions data, along with the methodologies applied to calculate emissions, to regulatory bodies (e.g., the EU) or voluntary programs (e.g., UNEP OGMP 2.0). Verification refers to the process of validating emissions across the supply chain and providing verified results for both total emissions and intensity from production.⁵⁻⁷

To date, MMRV remains an ongoing effort, and equivalent frameworks are also being adopted by voluntary initiatives, such as the Oil and Gas Methane Partnership (OGMP) 2.0, the MiQ standard, and Veritas 2.0.⁸⁻¹⁰ Some regulatory initiatives, including Air Quality Control Commission Regulation 7, Part B, implemented by the Colorado Department of Public Health and Environment [e.g., ref 11], have also incorporated similar frameworks. The key objectives of integrating MMRV into emissions reporting and management include guiding the development of measurement technology, establishing an internationally recognized standard to enhance the credibility of emissions reporting, enabling better reconciliation between emissions estimates from bottom-up (BU) and top-down (TD) approaches, creating a more accurate inventory, and generating credible assessments of overall carbon intensity across the supply chain.⁷

Various technical challenges and inherent emissions characteristics hinder the effective implementation of MMRV by O&G operators. These challenges include missing emissions from abnormal events in emissions reporting, limited availability of measurement data that captures routine operational events, insufficient temporal and spatial coverage of remote O&G sites, undocumented operational activities, inaccuracies in emissions attribution, and difficulty in unifying multi-scale emissions data.^{5, 12-14}

To address these challenges and generate a more accurate emissions estimation, the scientific community has been actively developing hybrid approaches that integrate both BU and TD data to maximize the utilization of emissions data. This includes combining measurement results through multi-scale remote sensing technologies, applying advanced statistical methods to create measurement-informed inventories, and developing simulation approaches.¹⁵⁻²² However, no data integration methodology or data model has been developed to spatiotemporally assimilate emissions data from different measurement scales and estimate annual emissions along with their associated uncertainty estimates.

This work introduces a novel event-based framework that utilizes the Emissions Event Data Model (EEDM), designed to spatially and temporally integrate multi-scale emissions measurements with O&G operational data. The model is developed based on the International Organization for Standardization (ISO) 19156:2023 and the Open Geospatial Consortium (OGC) 20-082r4 standards, integrating with the OGC Sensor Web Enablement suite.^{23,24} In the following sections, we first introduce EEDM and three types of emissions events. Next, we outline the methodology for calculating emissions and the associated uncertainties for each type of emission event. Third, we present two Monte Carlo approaches for estimating total emissions from unmeasured events

(defined as unresolved events in our framework). Finally, we present two case studies to demonstrate our framework using synthetic emissions data from upstream O&G sites.

2. Method and Materials

2.1 Emissions Event Data Model (EEDM)

Conventionally, methane emission data are modeled and managed for each emissions observation (EO). This process captures any form of detection, null-detection, or operational data indicating the presence or absence of CH₄ pollutants in the atmosphere, along with the timing (when) and location (where) of emissions, as well as the quantity (how much) emitted. This EO will be attributed to a specific physical source or activity depending on the scale and cause (e.g., fugitive emissions, tank venting, liquid unloading, etc.). However, EOs are typically discrete in time and space, captured at different scales (e.g., site, equipment, component; [e.g., ref 25]), and quantified using different algorithms. For example, snapshot emission observations, such as aircraft flyover measurements, provide a more accurate quantification of emissions from a specific site or piece of equipment. An Optical Gas Imaging camera pinpoints a leak from a component (e.g., a valve). In contrast, continuous monitoring systems have lower detection limits and are capable of measuring both the rate and duration of emissions. The characteristics and differences between these technologies make it challenging to unify them.

To address the challenges, an event-based framework (Figure 1a) and an emissions event data model (EEDM; Figure 1b) were proposed based on the OGC standards, including ISO/OGC's Observations and Measurements 19156:2023/OGC 20- 082r4.^{23,24} EEDM consists of five primary classes, which are emissions observation (EO), duration, source, course, and quantity.

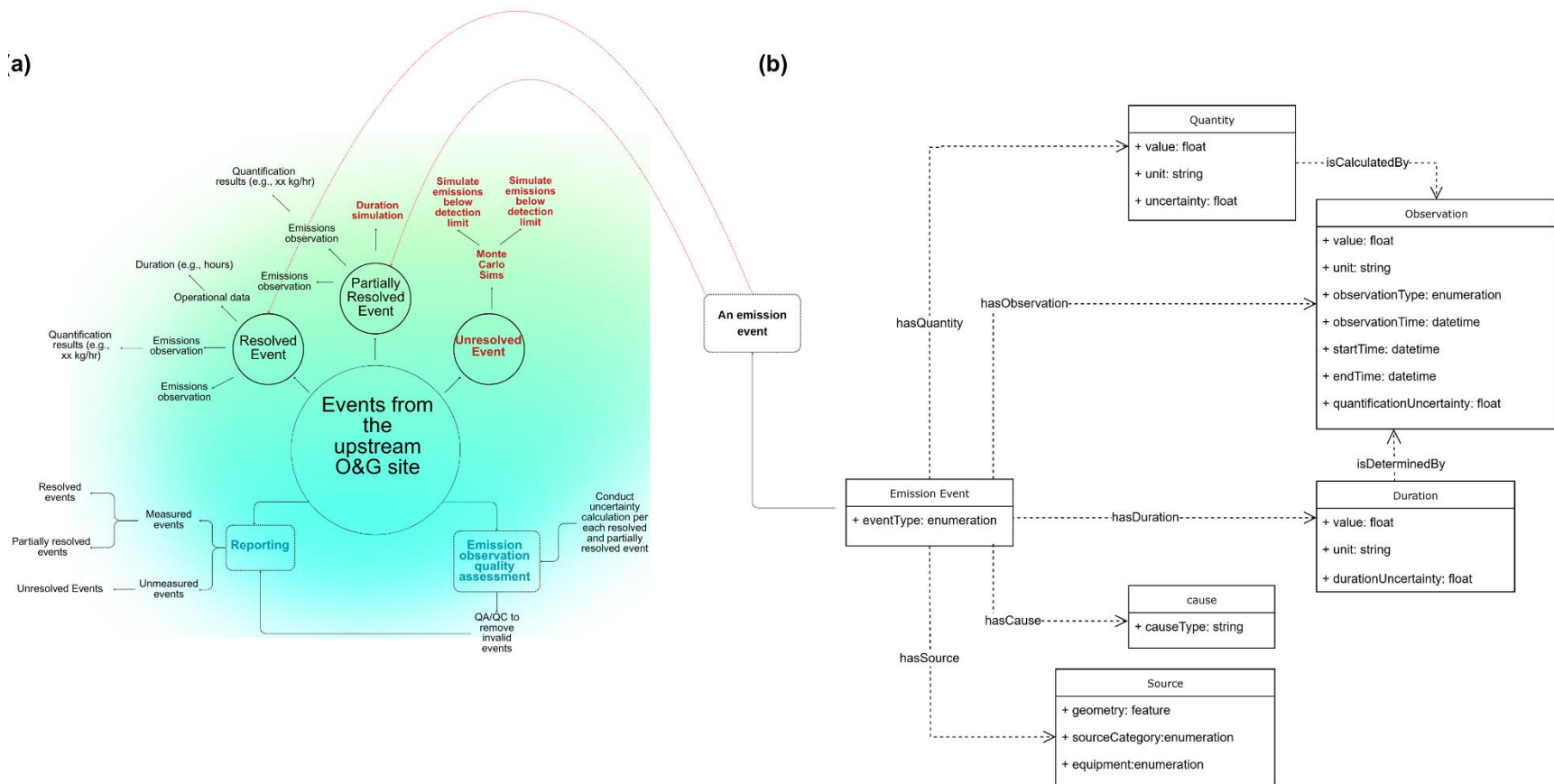


Figure 1. (a) Schematic view of event-based framework; **(b)** The entities and properties of the EEDM and their relationships. The UML definition of EEDM can be found in S1 of the Supporting Information (SI).

2.2 Spatial and Temporal Correlation of Emissions Event (EE)

An emission event (EE) may consist of either a single EO or multiple EOs (Figure 1a). We use spatial association [e.g., ref 26] and Allen's interval algebra [e.g., ref 27] to determine whether multiple EOs can be grouped into the same event and resolved both spatially and temporally. Spatial association assesses whether two or more EOs observe the phenomenon or feature of interest.²⁶ In this case, the geographical location associated with the feature of interest (i.e., latitude and longitude) should be the same or close. If the coordinates are not available, two EOs should be attributed to the same source (e.g., Compressor No. 1) or carry the same location indicator with the same scale (e.g., facility ID, 001).

Temporally, Allen's interval algebra (Table S1) is used to determine the temporal relationships between EOs. In total, thirteen fundamental temporal relationships are defined: *precedes*, *preceded by*, *meets*, *met by*, *overlaps*, *overlapped by*, *contains*, *during*, *starts*, *started by*, *finishes*, *finished by*, and *equals*.²⁷ Except for the "precedes" and "precededBy" relationships, if any two or more observations satisfy any of the other eleven relationships and are also spatially close (or attributed to the same equipment), they are more likely to originate from the same emission within the same emission event. The *precedes* and *precededBy* describe the intermittency (i.e., emissions that are stopped and started again). In this framework, we treat intermittent emissions as separate events.

The source refers to equipment that emits methane or activities that lead to emissions. An EO can be attributed to a specific physical source (e.g., Compressor No. 1), a source category (e.g., fugitives), or both (e.g., hydraulic fracturing from a gas well). The cause of an emission event is tied to the results of a root cause analysis, such as *the thief hatch was forgotten to close*. All observations within the same event should share a common cause and source. Each EO has its quantification result, associated unit, type of observation (e.g., aircraft flyover - Bridger), observation time, which describes when the observation was conducted, and start and end times if the observation is reported as a period, as well as quantification uncertainty (e.g., $\pm 40\%$, 10 kg/hr or [-5, 10] kg/hr).

The duration of EE can be obtained either directly from the operational data (e.g., scheduled venting from 10:00 am to 10:15 am), based on measurements from CMS (e.g., start and end times of alarms) or estimated indirectly through observation results, such as the absence of emissions or null detection. Finally, the quantity represents the total amount of methane emitted during the event. The generic equation for calculating the quantity of emissions events is rate times duration (see Eq. 2). When an event comprises multiple measured emissions observations or multiple quantification results, the rate of observation with the lowest quantification uncertainty is chosen for the event rate. For scheduled operational events, emissions can be derived from engineering calculations, such as Equation W-7A from 40 CFR Part 98, Subpart W [e.g., ref 28], calculating emissions from a single-well liquid unloading. Since uncertainty from engineering calculations is significantly tied to the equation being used and varied by regulation, our framework focuses on

uncertainty from measured emissions for now. The overall uncertainty of the measured emissions quantities results from error propagation from both quantification results and duration estimation.

2.3 Resolved Event, Partially Resolved Event, and Unresolved Event

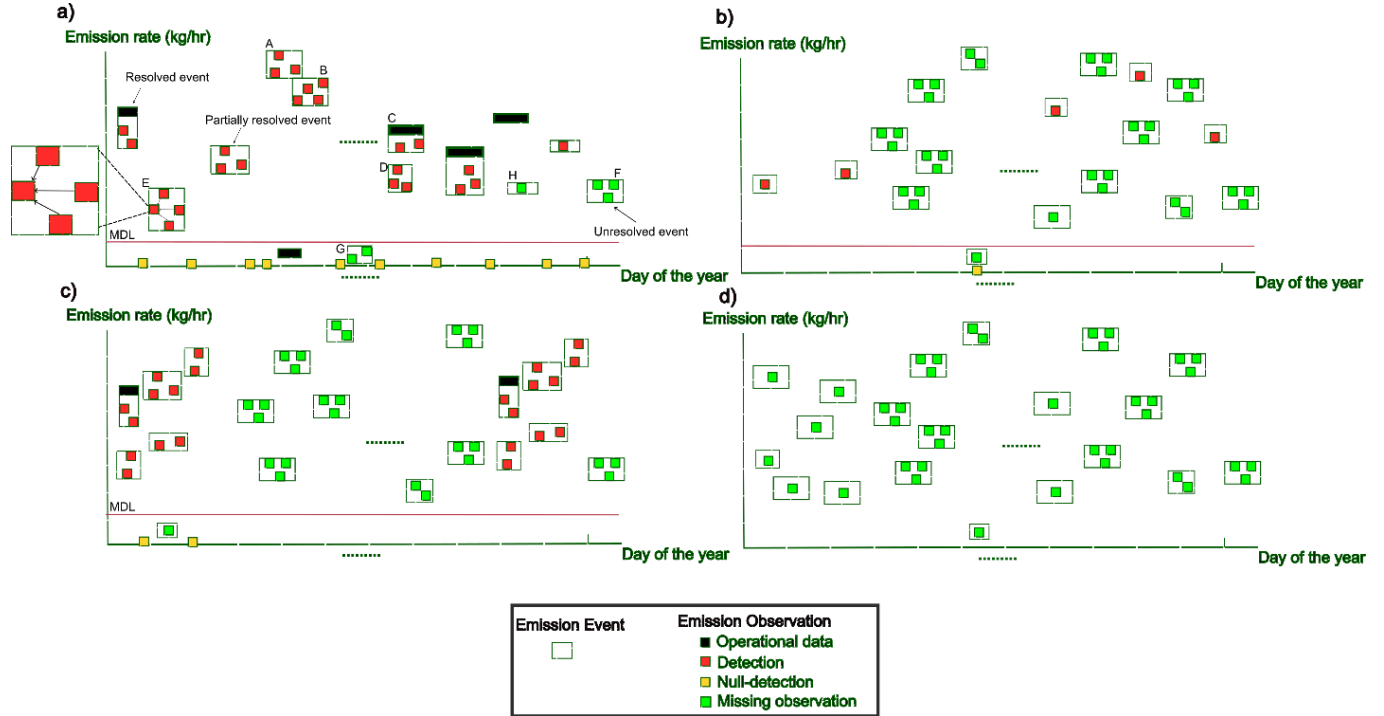


Figure 2. Representation of resolved, partially resolved, and unresolved emission events for four sites under different monitoring scenarios throughout the year. The x-axis and y-axis describe the emissions rate and time of the year, respectively. The scatter represents the three types of emissions observation (EO). The red square is the detection from any technology; the black square represents the operational event scheduled at a given time period; the yellow scatter represents the null detections; and the green square indicates a finite number of missing observations that have never been measured or recorded. By following the spatial association and Allen's interval algebra, EOs can be grouped into events, which are represented by using the green rectangle with width indicating the duration of the event and height indicating the range of rate (\pm uncertainty) of the event. Based on the temporal coverage, events are listed in chronological order. (a) A site with CMS measuring emissions 24 hours a day; (b) A site monitored through flyover surveys conducted every few months; (c) A site with a measurement campaign in which emissions are only measured during the campaign; and (d) A site without any monitoring or measurement.

Table 1: Three categories of emission event types.

Emission Event Type	Definition	Duration Determination	Emissions Quantity from Events	Uncertainty
Resolved Event (RE)	Events with durations determined using operational data/log	Extracted from operational data/log	Calculated	Only quantification uncertainty is considered
Partially Resolved Event (PRE)	Events with duration that are either measured by remote sensing technologies or estimated using null-detection and rules	Simulated by using proceedings and succeeding null-detection times	Calculated	Quantification uncertainty and duration estimation uncertainty
Unresolved Event (UE)	Events that are missing from annual emissions data	Simulated	(1) Simulate emissions that are not detected using POD checks (2) Simulate emissions by random sample RE and PRE	Estimated in the simulations

As shown in Figure 1a, we classify EE into three types: resolved events (REs), partially resolved events (PREs), and unresolved events (UEs). Table 1 presents the definitions and differentiations of each type of EE within our framework. REs include EOs from data sources such as operational logs, which typically contain information on duration, known emissions sources (for scheduled events), and causes. In contrast, PRE consists of EOs from only measurement technologies. They may require additional information to determine their duration, source, and cause, such as estimating duration using data from routine leak detection and repair (LDAR) surveys that do not identify emissions. The unresolved events (UEs) represent all other unmeasured and undocumented emissions and can be further classified into three types:

- **Type 1** occurs when emissions are present, but their rate falls below the deployed technology's minimum detection limit (MDL) (e.g., event G in Figure 2a). This type of UE, also known as a false negative, represents an undetected emission event.
- **Type 2** happens when no measurement technology is deployed to detect the emission (e.g., event F in Figure 2a).
- **Type 3** occurs when a small fugitive emission coincides with a large operational event (e.g., event H in Figure 2a) from the same equipment. Emissions from Type 3 events are typically small and are often omitted because fugitive measurements will not be conducted during the operational event.

Based on the above definitions, we can define the three types of EE mathematically based on the following expressions:

Let:

E be the set of all emission events.

RE , PRE and UE be the subsets of E corresponding to Resolved Events, Partially Resolved Events, and Unresolved Events, respectively.

EO_m be the set of emissions observations from measurement technologies.

EO_o be the set of emissions observations from operational logs.

N be the set of null-detection data (including from screening survey or LDAR inspection).

U be the set of emissions data that are not captured by any emissions observations.

Then we can define each emission event type as:

For resolved events (REs):

$$RE = \{e \in E \mid e \text{ has at least one observation from } EO_o\}$$

For partially resolved events (PREs):

$$PRE = \{e \in E \mid e \text{ has at least one observation from } EO_m \text{ but lacks } EO_o\}$$

For unresolved event (UEs):

$$UE = \{e \in E \mid e \notin RE \cup PRE\} = \{e \in E \mid e \text{ has no observation from } EO_m \text{ or } EO_o\}$$

To ensure that every EE falls into exactly one category:

$$E = RE \cup PRE \cup UE,$$

$$RE \cup PRE = \emptyset,$$

$$RE \cup UE = \emptyset,$$

$$PRE \cup UE = \emptyset,$$

To ensure that each physical emission source (i.e., equipment) has a unique event within each period, we reapply spatial association and Allen's interval algebra to merge events. For example, event A and event B can be merged if event A overlaps with event B. Likewise, event C and event D can be merged if event C contains event D, as illustrated in Figure 1a. After merging, the duration and quantity are recalculated by using the same rule. By following the structure of RE, PRE, and UE, annual emissions from an upstream site (E_{Total}) can be calculated as follows:

$$E_{Total} = \sum_{i_{RE}=1}^{N_{RE}} E_{RE_i} + \sum_{i_{PRE}=1}^{N_{PRE}} E_{PRE_i} + \sum_{i_{UE}=1}^{N_{UE}} E_{UE_i} \quad Eq. 1$$

where N_{RE} , N_{PRE} and N_{UE} indicates the number of resolved, partially resolved, and unresolved events, respectively. The E_{RE} , E_{PRE} , and E_{UE} represents total CH₄ emissions quantity from each resolved, partially resolved, and unresolved event, respectively.

Based on how measurement technologies are deployed on-site, an upstream O&G site can be measured or monitored under the following scenarios:

- **Instantaneous screening technology and continuous monitoring systems:** If operational events are reported and both instantaneous screening technology and continuous monitoring systems are deployed at the site (Figure 2a), then the annual emissions quantity can be calculated using all three types of EE.
- **Instantaneous screening survey only:** If a site has only been surveyed using snapshot measurement technologies, such as bi-monthly flyovers (Figure 2b). In that case, no REs are available and total emissions from E_{RE} are zero; instead, emissions from REs will be simulated as E_{UE} (e.g., uncaptured abnormal events). Thus, annual emissions are calculated by summing E_{PRE} and E_{UE} .
- **Measurement campaign only:** If a site has only been surveyed during an annual or biannual measurement campaign (Figure 2c) and emissions are also only reported during the measurement campaign, only a limited number of REs and PREs are measured during the campaign. Thus, E_{UE} needs to be simulated for periods outside the measurement campaign.
- **No Emissions data available:** If a site has no measurements at all (Figure 2d), both E_{PRE} and E_{RE} are zero, and E_{UE} needs to be simulated for the entire year (or reporting time range).

2.4 Generic emissions estimation equation for EE

The generic equation of calculating emissions quantity (E) of an event can be described as follows:

$$E = Q \times D \quad Eq. 2$$

where Q and D are emission rate and duration of the event.

2.5 Resolved Event (RE)

For REs, the uncertainties associated with each event primarily arise from uncertainties in rate estimation. While operational data can be used to estimate event durations, the associated uncertainties are challenging to estimate and exhibit significant variability across different operational practices.²⁹ Thus, we omit duration uncertainty for REs. However, quantification uncertainty should be accounted for, either by utilizing uncertainty estimates provided by technology vendors or by simulating or calculating it through engineering methods. By incorporating the quantification uncertainty (U_{Q_RE}), the emissions quantity estimation of a RE (E_{RE}) can be expressed as follows:

$$E_{RE} = Q_{RE} \times D_{opt} \pm U_{Q_RE} \times D_{opt} \quad \text{Eq. 3}$$

where the emission rate (Q_{RE}) is obtained either from engineering calculations or quantified using measurement technology, along with the associated quantification uncertainty (U_{Q_RE}). The duration (D_{opt}) is associated with operational data. Therefore, the uncertainty of emissions quantity of RE (U_{E_RE}) can be calculated by multiplying the quantification uncertainty by the operational duration. Eq. 3 can also be rewritten as follows:

$$E_{RE} = Q_{RE} \times D_{opt} \pm U_{E_RE} \quad \text{Eq. 4}$$

It should be noted that some engineering equations directly calculate emissions quantity (E_{RE}). In such cases, the uncertainty should be determined based on the equation used in the calculation.

2.6 Partially Resolved Event (PRE)

Unlike REs, the uncertainty of PREs must account for both quantification and duration uncertainties. For PREs that include observations from CMS, start and end times are typically measured based on the time when CH₄ concentration exceeds the background methane concentration. However, studies have shown that the measured durations can differ significantly from actual durations, and a Probabilistic Duration Model has been proposed to address this issue.^{30,31} In contrast, the duration of PREs constructed from instantaneous emissions observations is often estimated using rules or times derived from non detections [e.g., ref 32]. As a result, these duration estimates may either overestimate or underestimate actual durations.

To improve duration accuracy for this type of PRE, we developed an event-based Monte Carlo simulation workflow that integrates the process of leak production and natural repair in stochastic emissions models [e.g., ref 33,34] and the preceding null detection (PND) and succeeding null detection (SND) times of a given detection to estimate the duration and associated uncertainty of an event.

As shown in Figure 3, a Monte Carlo simulation (10^5 iterations) is performed to simulate the duration and ensure the stationary distribution of the results. The start and end times of the simulation were bounded by PNDT and SNTD, respectively. Each simulation iteration initializes the emission event as "not occurring." To determine the start time of the emission event, the simulation randomly samples from a binomial distribution created based on an emission probability calculated using the LPR equation.³³ If an emission is sampled, the simulation's timestamp becomes the start time of the emission event. The simulation updates the event's status to "ongoing" and proceeds to the next day. Otherwise, the simulation directly proceeds to the next day and repeats the sampling process. Once an emission event is ongoing, a second binomial distribution, created based on a probability calculated using the NRR equation from Fox et al.³³, is used for sampling to determine when the event will cease. If the event is stopped, the simulation timestamp is saved as the event's end time; otherwise, the process continues to the next day until the timestamp exceeds the SNTD. At the end of each simulation run, (1) the simulated end time is set to the SNTD if the emission event remains ongoing, and (2) If no emission event occurred during the simulation, the simulated start and end times are set to the PNDT and SNTD, respectively.

The simulated duration (D_{sim}) is then calculated as the difference between the simulated end and start times. After 10^5 iterations, the median simulated durations ($\overline{D_{sim}}$) and 2.5- ($D_{sim_2.5\%}$) and 97.5-percentiles ($D_{sim_97.5\%}$) of simulated durations are used to represent the duration and uncertainty of PRE.³⁵

By integrating both the uncertainty from duration estimation and the uncertainty from quantification (U_{E_PRE}), the emissions quantity of each PRE (E_{PRE}) can be calculated by using the below equation:

$$E_{PRE} = Q_{PRE} \times D_{PRE} \pm U_{E_PRE} \quad Eq.5$$

where the D_{PRE} can be either calculated or simulated:

$$D_{PRE} = \begin{cases} T_{end} - T_{start}, & \text{if determined using CMS measurement} \\ \overline{D_{sim}}, & \text{if determined using null detect or rule} \end{cases} \quad Eq.6$$

U_{E_PRE} represents uncertainties associated with the emissions quantity estimated for each PRE. It consists of both quantification uncertainty ($U_{Q_{PRE}}$) and duration estimation uncertainty ($U_{D_{PRE}}$), which can be calculated as follows:

$$U_{D_{PRE}} = \begin{cases} PDM(T_{end}, T_{start}, C_{CH4}), & \text{if determined using CMS measurement} \\ [D_{sim_2.5\%}, D_{sim_97.5\%}], & \text{if determined using nondetect or rule} \end{cases} \quad Eq.7$$

Where $PDM(T_{end}, T_{start}, C_{CH4})$ is the duration uncertainty estimated by using method proposed by Daniels et al.³¹.

To combine uncertainties from quantification and duration estimations, the error propagation equations described by IPCC³⁶ are used to calculate U_{E_PRE} :

$$U_{E_PRE} = \sqrt{(U_{Q_PRE})^2 + (U_{D_PRE})^2} \quad Eq.8$$

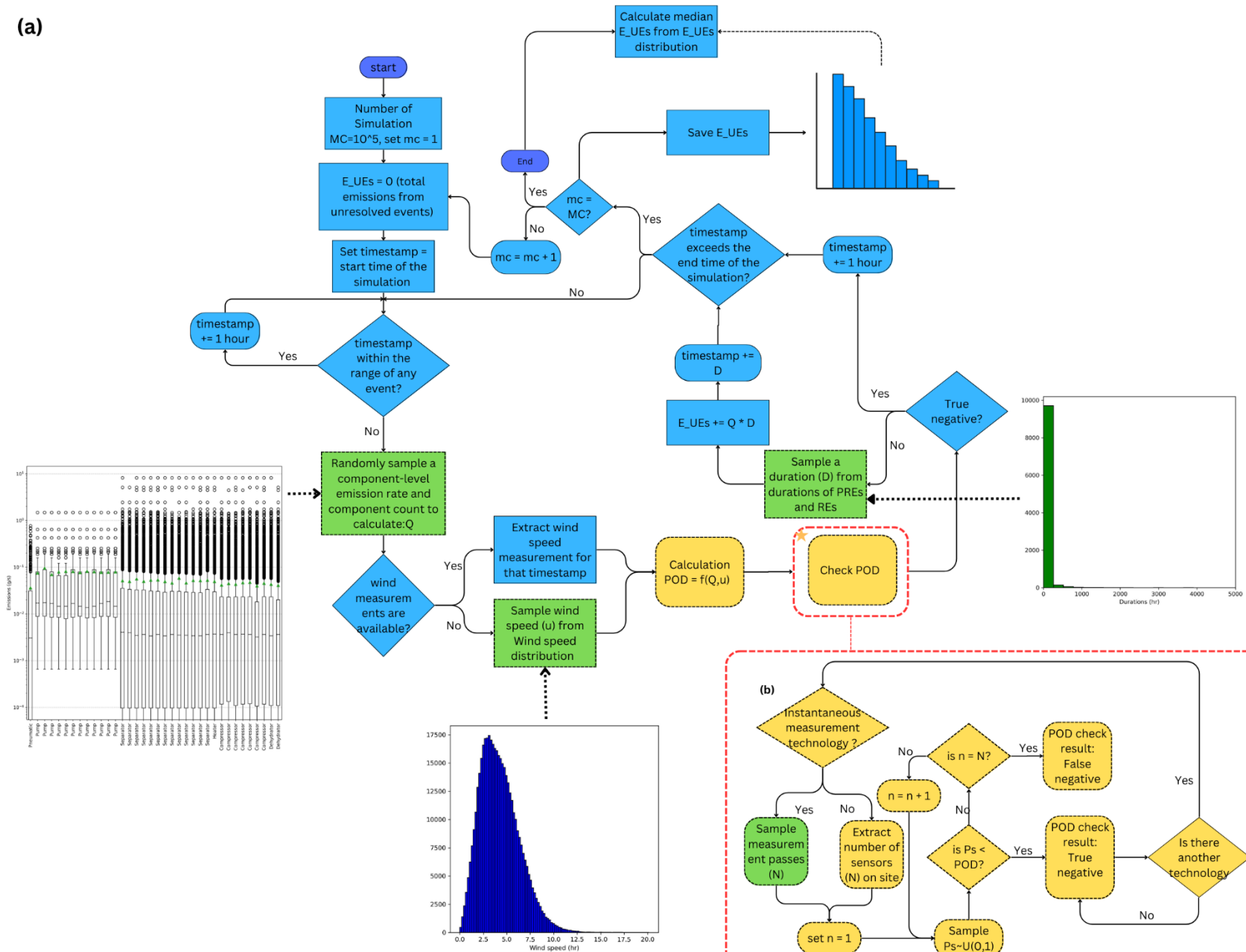
The *Eq.8* assumes that duration estimation uncertainty and quantification uncertainty are uncorrelated. However, when PRE's duration is measured by CMS, the rate and duration may correlate since they are typically generated from the same algorithm and sensor. While this correlation is important, a detailed investigation is beyond the scope of this study.

2.7 Estimating emissions and uncertainty from UEs

We developed two distinct simulation approaches to estimate emissions from UEs at a given site. The first simulation integrates a published methodology from Johnson et al.¹⁶ into the event framework, using a probability of detection (POD) equation and a stochastic process to identify UEs below the minimum detection limit (MDL) of the deployed technologies. The second simulation addresses scenarios in which measurements are insufficient to calculate the annual emissions of a given site (e.g., the third and fourth scenarios in Figures 2c and 2d). Instead of relying on POD, it simulates UEs based on the likelihood of emission event occurrence and precalculated expected emissions rate and duration distributions.

2.7.1 Simulating Emissions from UEs using probability of detection (POD)

(a)



(b)

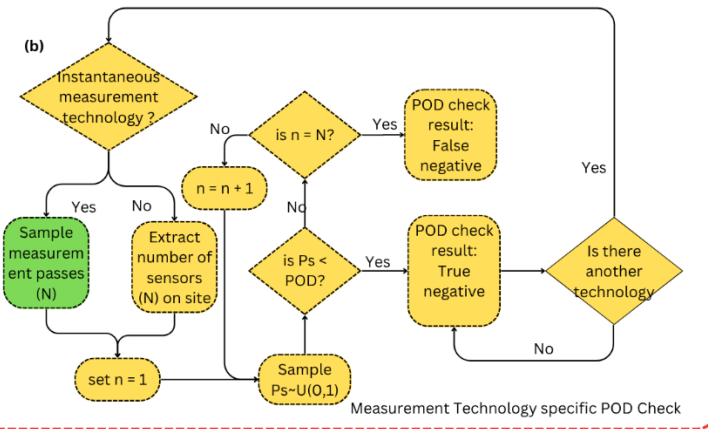


Figure 4. Monte Carlo simulation workflow to estimate total emissions from unresolved events for a given site that is monitored by flyover and CMS. This workflow illustrates a specific scenario in which both aircraft flyovers and CMS are deployed to measure emissions. Each probability of detection (POD) check is independent of the others. Therefore, additional checks are necessary when more than two technologies are deployed for emission monitoring. ^aComponent-level emissions distributions should be derived from real measurements, such as dataset summarized by Rutherford et al.²⁰. ^bDifferent aircraft systems require different equations to calculate POD based on different parameters. For instance, Conrad et al.³⁷ provided POD equations for three different aircraft systems. Here, the flowchart only assumes the POD is affected by wind speed. ^cSimilarly, Bell et al.³⁰ derived POD equations for multiple CMSs in METEC based on a single-blind test. ^dThe duration distributions are based on empirical data from partially resolved events (PREs) of the site (or sites with similar characteristics if site clustering analysis is correctly performed).

As illustrated in Figure 4, the simulation workflow begins by initializing the simulation time to the start of the reconciliation period (usually the first day of the year, such as 2024-01-01T00:00:00 for the annual reconciliation) and setting possible emissions from UEs ($E_{UE_{sim}}$) to 0. At each hourly timestep, the simulation checks if the current timestamp falls within the range of any emission event (both RE and PRE). If the timestamp exceeds the simulation range (e.g., the last day of the year, such as 2024-12-31T23:59:59), the simulation proceeds to the next iteration. When timestamp in simulation time is not included by any REs and PREs, meaning a potential UE may occur, a component-scale emission rate and component counts are sampled from either the inventory or database containing component-scale measurements to obtain an equipment- or site-scale emission rate. Next, wind speed and flight passes for each flyover survey at the site location are also randomly sampled. The former is used to calculate POD, and the latter is used to determine the number of survey attempts.

Subsequently, the simulation determines the false negative and identifies whether any measurement technology fails to detect an emission independently for each survey attempt. A calculated POD is then compared to a randomly generated probability (ξ) between 0 and 1. If the POD exceeds ξ , it indicates a false negative (i.e., if the UE occurred in the real world, it would not have been detected). If the POD is smaller than ξ , it indicates a true negative (i.e., if the UE occurred in the real world, it would have been detected). This comparison is conducted for each flyover path and each sensor installed on the site. If either the flyover or CMS POD check indicates a false negative, the sampled emission rate is multiplied by a sampled duration to consolidate the emissions quantity of the sampled UE. Then, the simulated emissions quantity is added to the cumulative $E_{UE_{sim}}$. The sampled duration is also added to the timestamp in the simulation. If POD checks from flyover and CMS both return true negative, meaning no emissions occurred at the time step, the simulation proceeds to the next hour. This process is repeated until the timestamp exceeds the simulation period. Then, the Monte Carlo counter is incremented, and we repeat the whole process until 10^5 iterations are completed. Finally, the median ($\bar{E}_{UE_{sim}}$) and the 2.5th and

97.5th percentiles of the $E_{UE_{sim}}$ distribution are calculated across all simulation iterations to represent the simulated emissions from UEs and their uncertainty.

2.7.2 Simulating Emissions from UEs using probability of emission event occurrence

Identifying false negatives from a site requires sufficient temporal coverage of emissions measurements (i.e., either through continuous monitoring systems or frequent instantaneous screening surveys). However, in reality, not all sites are monitored sufficiently. To address this challenge, we developed a second simulation approach that models UEs based on the probability of emission event occurrence rather than depending on the POD of deployed measurement technologies.

Prior to simulation, the following distributions are required to be created from the REs and PREs:

- The emission rate distribution (Q_{dist}) represents the expected emission rates for a given potential emission source category or equipment category.
- The emission duration distribution (D_{dist}) represents the expected durations for a given potential emission source category or equipment category.
- The probabilities represent the likelihood of an emission event occurrence ($P_{occurrence}$) and not occurrence ($P_{not_occurrence}$) for a given potential emission source category or equipment based on D_{dist} . Since multiple pieces of equipment can emit simultaneously and the emission of one piece is independent of another, sites with more equipment are more likely to have a higher probability of emissions occurring.

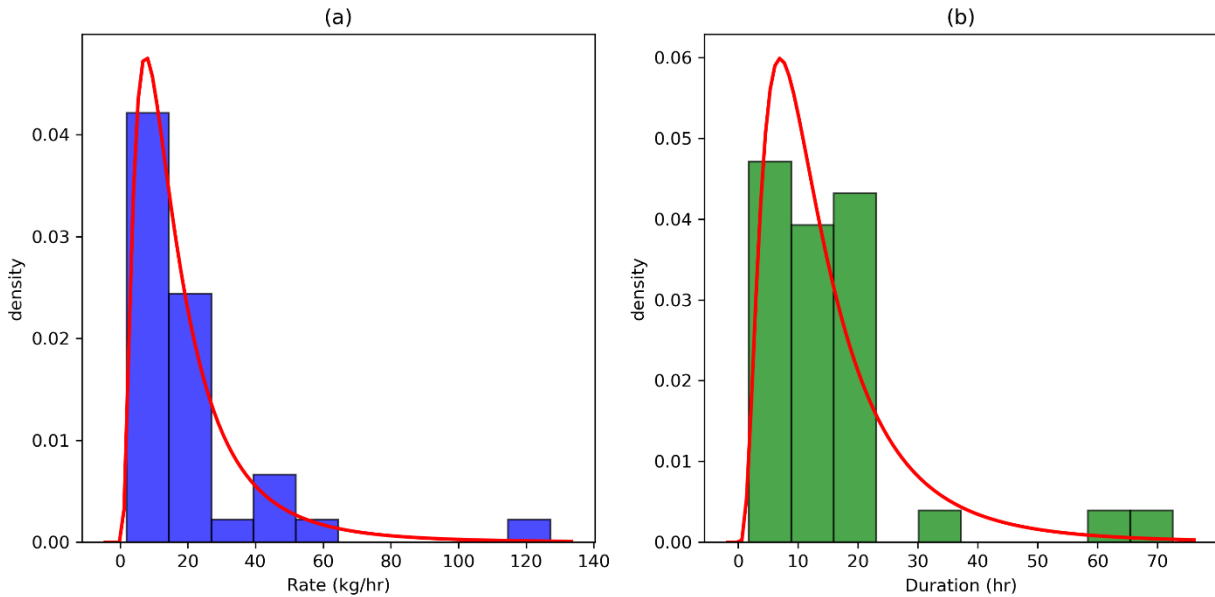


Figure 5. Example of using *Eq.9* to fit empirical rate (a) and duration (b) distributions. The histogram represents the rate and duration of REs and PREs. The red curve represents the best-

fitted function based on the distributions. By using the red curve, the expected emissions rate and duration distribution can be created.

Since emission rates and durations tend to follow right-skewed distribution, we use a log-normal probability density function to fit the empirical measured Q_{dist} and D_{dist} from REs and PREs (as shown in Figure 5).

$$P(v) = ae^{v^b} \quad Eq.9$$

Where v is the rate or duration sampled under the probability $P(v)$, and a and b are parameters required to fit the rate and duration for each source category or equipment type.

After fitting, the log-normal PDF with optimal a and b are used to create the expected rate and duration distributions, Q_{exp_dist} and D_{exp_dist} , for UEs.

The probability of emission event occurrence ($P_{occurrence}$) can be calculated by using: $\frac{\text{total duration from REs and PREs}}{\text{total observation period}}$. Then the probability of no emission event ($P_{not_occurrence}$) can be calculated by using: $1 - P_{occurrence}$. To sample an event a binomial distribution can be created based these two probabilities.

$$B(x) = \binom{n}{x} P_{occurrence}^x P_{not_occurrence}^{n-x} \quad Eq.10$$

Where x is the proportion of time that a source can have an emission event in a given period (n). Since the probability is calculated using duration, $P_{occurrence}$ and $P_{not_occurrence}$, it also describes how frequently a source can have an emission event.

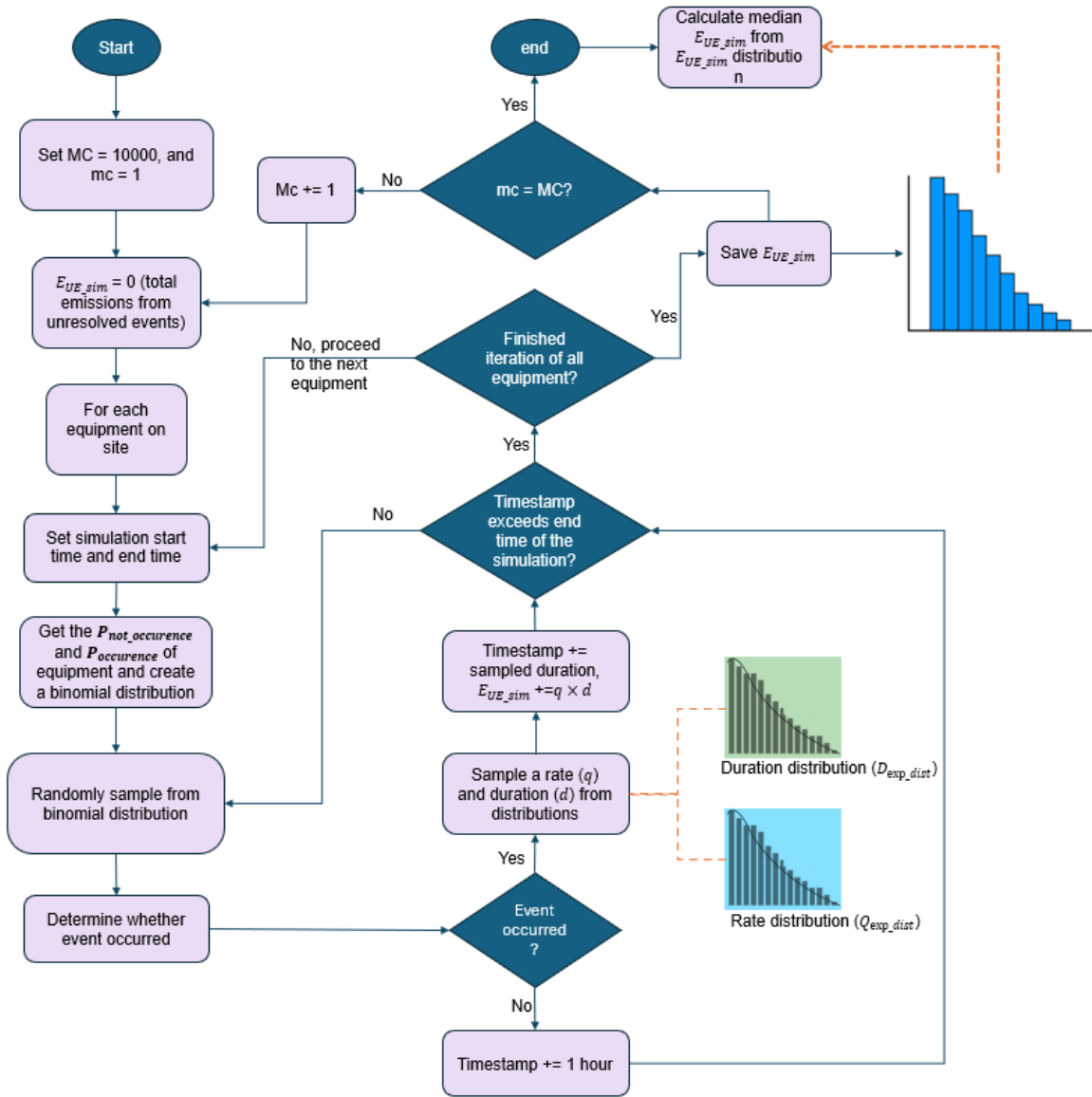


Figure 6. A workflow of simulating emissions from UEs based on the probability of event occurrence and expected rate and duration distributions.

The event occurrence simulation is also a Monte Carlo approach. It begins by setting the timestamp to the start of the year and initializing emissions from UEs (E_{UE_sim}) to 0 kg. The simulation proceeds hourly and determines the event occurrence by sampling from the binomial distribution created based on the precalculated $P_{occurrence}$ and $P_{not_occurrence}$. If an emission occurs, the emission rate (q) and duration (d) are sampled from the expected rate (Q_{exp_dist}) and duration (D_{exp_dist}) distributions, respectively, to define a UE. The E_{UE_sim} then updated by adding $q \times d$, and the simulation time is incremented by d . If no emission event occurs, the simulation time

advances by one hour. This event sampling is repeated for each piece of equipment until no emissions are confirmed from all equipment on site.

This process is repeated until the end of the simulation time (i.e., end of the year). The E_{UE_sim} is calculated by summing emissions from all sampled UEs. The simulation is repeated for 10^5 iterations, and the median (\bar{E}_{UE_sim}), along with the 2.5th and 97.5th percentiles of all E_{UE_sim} , are calculated to represent the simulated emissions from UEs and their associated uncertainty.

For this methodology, equipment data and bottom-up inventory are essential to improve the simulation results, avoid extrapolating emissions from inaccurate or nonexistent source categories and ensure the sampling mechanism aligns with the site's infrastructure and activities. For example, events from the separator (i.e., REs or PREs that are attributed to the separator) should not be used to create the expected rate and duration distribution if the site does not have separators.

2.8 Estimating emissions and uncertainties across all EEs

By integrating the simulated emissions from UEs (\bar{E}_{UE_sim}), Eq. 4 and Eq. 5 into Eq. 1, it can be rewritten as:

$$E_{Total} = \sum_{i_{RE}=1}^{N_{RE}} Q_{RE_i} \times D_{opt_i} + \sum_{i_{PRE}=1}^{N_{PRE}} Q_{PRE_i} \times D_{PRE_i} + \bar{E}_{UE_sim} \quad Eq.11$$

By following the uncertainty equation suggested by IPCC³⁶, the uncertainties associated with emissions quantity of all REs (U_{E_RES}) and PREs (U_{E_PRE}) can be expressed as follows:

$$U_{E_RES} = \frac{\sqrt{(U_{E_RE_1} \times E_{RE_1})^2 + (U_{E_RE_2} \times E_{RE_2})^2 + \dots + (U_{E_RE_{N_{RE}}} \times E_{RE_{N_{RE}}})^2}}{|E_{RE_1} + E_{RE_2} + \dots + E_{RE_{N_{RE}}}|} \quad Eq.12$$

and

$$U_{E_PREs} = \frac{\sqrt{(U_{E_PRE_1} \times E_{PRE_1})^2 + (U_{E_PRE_2} \times E_{PRE_2})^2 + \dots + (U_{E_PRE_{N_{PRE}}} \times E_{PRE_{N_{PRE}}})^2}}{|E_{PRE_1} + E_{PRE_2} + \dots + E_{PRE_{N_{PRE}}}|} \quad Eq.13$$

where U_{E_RE} and U_{E_PRE} are calculated in Eq.3 and Eq.8, respectively.

By combining Eq 12-13, the total uncertainty (U_{E_total}) associated with E_{Total} can be calculated as follows:

$$U_{E_total} = \frac{\sqrt{(U_{E_RES} \times E_{RES})^2 + (U_{E_PREs} \times E_{PREs})^2 + (U_{E_RES} \times E_{UES})^2}}{|E_{RES} + E_{PREs} + E_{UES}|} \quad Eq.14$$

3. Case studies and results

To demonstrate our methodologies, we developed two distinct case studies to estimate total emissions from a fictitious site with ten pieces of equipment from January 1, 2024, to April 30, 2024. The first case study utilizes 146 simulated emission observations, including 89 CMS measurements, four flyover survey records (one of which did not detect any plume), four OGI inspection records (two of which did not find any leaks), and 49 venting data points. Due to the availability of sufficient EOs and the monitoring of all four months by CMS, we decided to simulate emissions from UEs using a POD-based approach. The second case study extrapolates emissions based on the probability of EE occurrence, using only 36 synthetic CMS observations spanning a single month. In this case, emissions from UEs are simulated based on the probability of an emission event occurring over three unmonitored months. Case Studies 1 and 2 correspond to Scenarios 1 (Figure 2a) and 3 (Figure 2c), respectively, as described in Figure 2. Tables S1 to S5 are synthetic emission observations for case study No.1, and Table S6 is the synthetic emission observations for case study No.2.

These two case studies demonstrate how annual emissions and their uncertainties can be estimated using the EEDM framework and its associated methodology. However, real-world applications may require adjustments to the parameters, equations, and simulation logic presented here. For example, it may be necessary to exclude certain months from simulations if sites are shut in during those periods to more accurately reflect operational realities.

3.1 Case study No.1

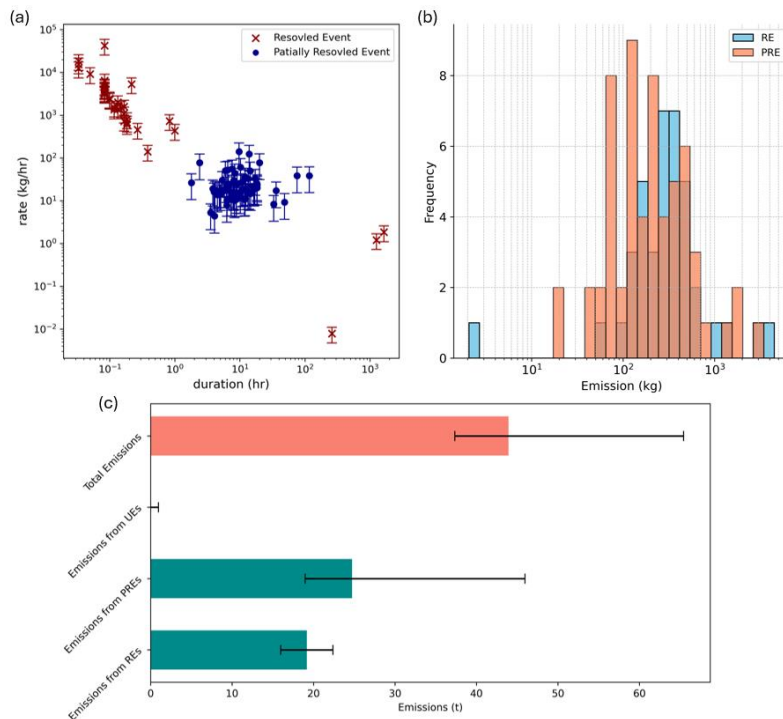


Figure 7. Results from the case study No.1: (a) Scatter plot of rates, durations, and associated uncertainties of REs and PREs after spatial association and Allen's interval algebra are applied; (b) Emissions quantities for REs and PREs after spatial association and Allen's interval algebra are applied (logarithmic scale); (c) The bar chart shows the total site-level emission estimates and breakdown of REs, PREs, and UEs emissions.

For case study No.1, we initiated 92 PREs and 49 REs. To demonstrate the proposed equations, we assume a quantification uncertainty of $\pm 60\%$ across all events. After merging the events, only one PRE requires duration simulation. The parameters and assumptions used to simulate the duration of this PRE include a default LPR of 0.006 leaks per day per site, a 7-day visitation interval, one leak per site at initialization, 10 global leaks, one active leak, and an operator bonus of 0.5. For the remaining PREs, durations were determined based on the measured start and end times from CMS observations. Following the findings from Daniels et al.³¹, the associated duration uncertainties of all CMS PREs are twice the measured duration.

After applying Allen's interval algebra and source attribution results, we merged 41 events, reducing the total number of events to 100, consisting of 61 PREs and 39 REs (Figure S1). The rate and duration distributions of both REs and PREs are skewed to the right with a weak correlation. The medians of rates and durations for REs and PREs are 2312.59 kg/hr and 0.1 hour and 18.53 kg/hr and 9.1 hours, respectively. However, events are clearly clustered, and their rate and duration are negatively correlated after both are converted to a logarithmic scale. As indicated in Figure 7a, all synthetic PREs (which contain only observations from either the flyover survey or CMS) vary between 0 and 100 kg/hr and persist for less than 1 hour to 4 days. The negative correlation indicates that most synthetic events have either a short duration or a low rate. It aligns with the findings from Wang et al.²², as the REs encompass operational data, which typically exhibit high emissions rates but shorter periods. Due to the right-skewed durations and rate distributions, without considering uncertainties, the top four REs and six PREs contributed to 47.9% and 42.1% of the total emissions quantities of REs and PREs, respectively (see Figure 7b).

The simulation of emissions below the MDL was applied to estimate total emissions from UEs. The following input parameters, datasets, and assumptions were used: five CMS sensors were installed on-site; wind speed data from the Permian Basin were downloaded from ERA5;³⁸ the flight passes were default to three passes; component-scale emission rates were sampled from empirical component measurements datasets published by Rutherford et al.²⁰; and POD equations of flyover system and CMS are accessed from Conrad et al.³⁷ and MIQ³⁹. The visualizations of input data for case study No.1 can be found in Figure S2.

Only one PRE had its duration estimated using proceeding and succeeding null detections. The resulting distribution of simulated durations was right-skewed (see Figure S3a), with a median duration of 115.75 hours and a 95% confidence interval (CI) of [4.75, 607.75].

Since both CMS and flyover are deployed for Case Study No. 1, the simulated emissions below the MDL of both technologies are significantly lower than the emissions quantities from RE and PREs (see Figure 7c). The median emissions quantities for all UEs are 31.73 kg (95% CI [3.34, 1016.00]; see Figure S3b).

Figure 7c illustrates the total emissions and breakdown emissions per each type of events. The total emissions over four months are 43.92 tonnes, with 95% CI [37.34, 65.41]. The breakdown of emissions from REs and PREs are 19.17 tonnes (95% CI [15.96, 22.38]) and 24.72 tonnes (95% CI [18.97, 45.95]).

3.2 Case study No.2

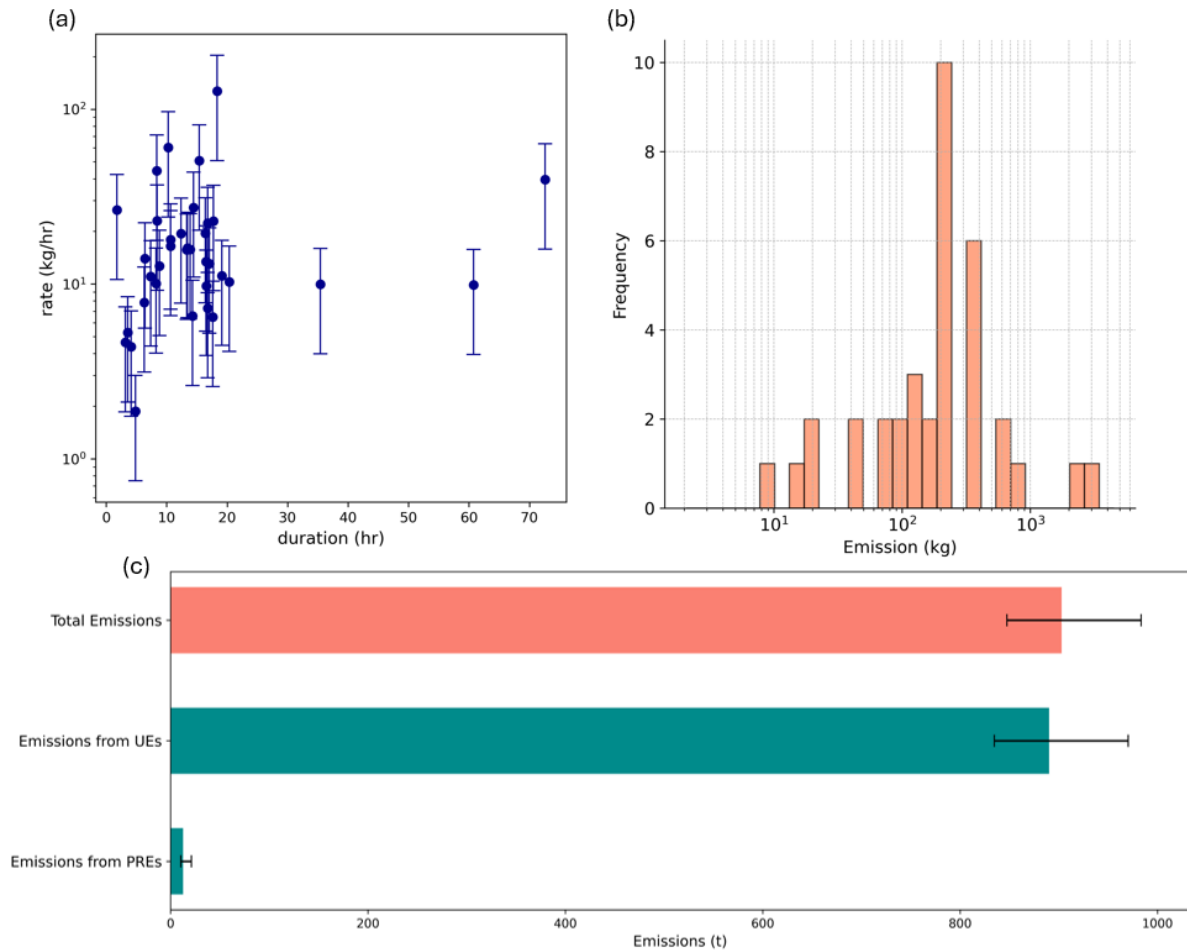


Figure 8. Results from case study No.2: (a) Scatter plot of rates, durations, and associated uncertainties of PREs; (b) Distribution of emissions quantities for PREs created using synthetic CMS emissions observations (logarithmic scale); (c) The bar chart shows the total site-level emission estimates and breakdown of PREs and UEs emissions.

In the second case study, 36 CMS synthesized observations over a month and initiated 36 PREs. Since all of them are neither spatially associated nor satisfy Allen's temporal algebra, no PREs are merged. These PREs are attributed to eight pieces of equipment from four different equipment types on our fictitious upstream O&G site (see Table S6).

Similar to Case Study 1, we assumed quantification and duration uncertainties of 60% and 0-200%, respectively. As shown in Figure 8a, no significant trend is detected between the rate and duration of synthetic PREs for case study No. 2. The medians of the rates and durations are approximately 13.71 kg/hr and 13.68 hours, respectively. By extracting rates and durations from REs, we created expected rate and duration distributions per each equipment type (see Figures S4 and S5). The emissions quantity distribution is right-skewed (see Figure 8b and 8c), with approximately the top four PREs contributing to 51.80% of total emissions (12.75 tonnes, with a 95% confidence interval (CI) of [10.32, 21.23]).

As shown in Figure 8c, by applying our proposed second simulation technique, the total simulated unmeasured emissions amount to 890.19 tonnes, with a 95% confidence interval (CI) of [834.60, 970.19]. This total includes 36.93 tonnes from Compressor-1, 36.80 tonnes from Compressor-2, 37.03 tonnes from Compressor-3, 27.60 tonnes from Dehydrator-1, 29.59 tonnes from Tank-1, 29.52 tonnes from Tank-2, 10.11 tonnes from Separator-1, 10.09 tonnes from Separator-2, 10.11 tonnes from Separator-3, and 80.85 tonnes from the Wellhead. The distribution of simulated unmeasured emissions for each piece of equipment is shown in Figure S6. Since the expected distributions are generated by equipment type, the simulated unmeasured emissions are nearly identical across different pieces of equipment of the same type. After adding the simulated emissions from UEs to the emissions from synthetic PREs, the total four-month emissions for our fictitious site are 903.29 tonnes, with a 95% CI of [847.30, 983.39].

4. Implication & Conclusion

We introduce an event-based framework and associated annual emissions estimation methodologies that integrate multi-scale measurements and oil and gas operational data to construct emission events. By adopting ISO and OGC standards, we ensure that emission events are generic across different scales of technologies. It highlights the following key implications:

- The EEDM represents a simplified data model developed in accordance with the ISO 19156, OGC 20-082r4, and the OGC Sensor Web Enablement suite of standards. It ensures basic compatibility and interoperability for assimilating sensor data across diverse measurement technologies. It supports quantification, duration estimation, source attribution, and cause analysis, which are usually four follow-up actions required for O&G operators to respond to emissions. A formal data model will be developed through collaborative group efforts.⁴⁰

- Differentiating between REs and PREs enhances uncertainty assessments. Previous studies indicate that many operational events are short duration events.²² Partitioning emissions from an intermittent source into several short-duration events can significantly reduce the overall uncertainties associated with estimating its annual emissions. Mathematically, most uncertainty in short-duration events arises from quantification rather than from both quantification and duration. Incorporating details of routine and non-routine operational activities into the emission event model can further enhance the accuracy of duration estimation.
- For PREs, although measurements from CMSs help decrease duration uncertainty compared to relying solely on snapshot screening technologies, such as aircraft systems, the duration uncertainty associated with CMSs also needs to be addressed. This is critical because surface wind directions often fluctuate on-site, particularly at locations with complex infrastructure.
- We integrated emission events into the methodology developed by Johnson et al.¹⁶, which is sensitive to the PODs of the deployed measurement technologies. Our case studies are based on POD equations derived for InsightM's aircraft flyovers and Qube's CMS. If other technologies are simulated, different POD equations should be used, and simulated UEs will also be different.
- Emissions extrapolation is generally required in two main scenarios: (1) sites with limited measurements and (2) sites with no events. For sites with limited measurements, accuracy is highly sensitive to the sample size of events (i.e., the number of REs and PREs) used to create the expected rate and duration distributions and to calculate probabilities. Both distributions are anticipated to improve as more events become available for fitting. Future research aims to determine the minimum number of events required to achieve relatively accurate simulation results. Site clustering analysis is often necessary to identify sites with similar characteristics, allowing accurately estimating emissions from unmonitored sites using events from monitored sites.
- In Case Study 2, distributions and probabilities can also be derived for individual activities or source categories to align with reporting frameworks, such as OGMP 2.0.
- The event model supports the creation of a measurement-informed inventory (MII) or measurement-based inventory (MBI) and is compatible with known voluntary initiative frameworks, such as Best-Measured vs. Best-Calculated from Veritas 2.0 and OGMP 2.0 Level 4 and 5 emissions reporting. REs and PREs can be grouped by source to aggregate events for each source category. For instance, the emission factor and its associated uncertainty for flaring can be calculated by dividing the total emissions from flaring events by the total number of flaring events and then dividing by the total duration of flaring events.
- Currently, our framework lacks a standard QA/QC process to validate input EOs. Adding such a standard in the future could ensure that only valid information is included in creating Ees.

This study presents an alternative framework for estimating annual site-level emissions in the upstream oil and gas (O&G) sector. By integrating multiscale emissions observations and operational data using EEDM, annual emissions and associated uncertainties can be estimated for each event by combining both quantified rates and estimated durations. The proposed framework has a substantial contribution to ongoing efforts aimed at creating a measurement-informed inventory, improving methane mitigation strategies, and supporting the global objective of reducing methane emissions in the O&G sector. Expanding the scope of our framework to include more types of methane emission and operational data (e.g., SCADA) and diverse operational conditions will further enhance its reliability. Future studies will also focus on demonstrating this methodology using real-world data across multiple sites to evaluate its feasibility and effectiveness on a broader scale.

Code and Data availability

The analysis was programmed in Python with standard packages. The results can be reproduced by employing the equations, explanations, and parameters provided in the main text. Additional code and data will be made available upon request

Declaration of Interest Statement

The authors declare that they have no known competing financial interests or personal relationships that could have appeared to influence the work reported in this paper.

Author contributions

M.G and S. L designed the research. M.G. directed and performed the analyses. M.G. and Z. A. wrote the paper. M.G., S.L., Z.A., S.S. and S. K. edited the paper.

References

- (1) IEA. *Global Methane Tracker 2023 – Analysis*. 2023. <https://www.iea.org/reports/global-methane-tracker-2023>.
- (2) UNFCC. *The Imperative for Methane Action*. 2021. <https://www.globalmethanepledge.org/imperative-methane-action>.
- (3) Directorate-General for Energy. *New EU Methane Regulation to reduce harmful emissions from fossil fuels in Europe and abroad*. 2024. https://energy.ec.europa.eu/news/new-eu-methane-regulation-reduce-harmful-emissions-fossil-fuels-europe-and-abroad-2024-05-27_en.
- (4) US EPP. *Methane Emissions Reduction Program and GHGRP Subpart W (Petroleum and Natural Gas Systems)*. 2024. <https://www.epa.gov/inflation-reduction-act/revisions-ghgrp-subpart-w-petroleum-and-natural-gas-systems>.

- (5) Allen, D.; Ravikumar, A.; Tullos, E. Scientific Challenges of Monitoring, Measuring, Reporting, and Verifying Greenhouse Gas Emissions from Natural Gas Systems. *ACS Sustainable Resource Management*, **2023**, 1(1), pp.10–12; DOI: 10.1021/acssusresmg.3c00132.
- (6) US Department of Energy. *Greenhouse Gas Supply Chain Emissions Measurement, Monitoring, Reporting, Verification Framework*. 2024. <https://www.energy.gov/fecm/greenhouse-gas-supply-chain-emissions-measurement-monitoring-reporting-verification-framework>.
- (7) US Department of Energy. *International MMRV Working Group Reaches Milestone in Developing a Credible Framework for Measuring Natural Gas Supply Chain Emissions to Drive Continuous Reductions in Methane and Carbon Dioxide Emissions in the Global Natural Gas Market*. 2024. <https://www.energy.gov/fecm/articles/international-mmrv-working-group-reaches-milestone-developing-credible-framework>
- (8) GTI Energy. *Veritas: Home*. <https://veritas.gti.energy/>.
- (9) MIQ. *The MiQ Standard*. <https://miq.org/the-technical-standard/>.
- (10) Oil and Gas Methane Partnership 2.0. *OGMP 2.0 – The Oil & Gas Methane Partnership*. <https://ogmpartnership.com/>.
- (11) Colorado Department of Public Health and Environment. *5 CCR 1001-9 REGULATION NUMBER 7 CONTROL OF EMISSIONS FROM OIL AND GAS EMISSIONS OPERATIONS*. 2025; <https://www.sos.state.co.us/CCR/DisplayRule.do?action=ruleinfo&ruleId=2341&deptID=16&agencyID=7&deptName=Department%20of%20Public%20Health%20and%20Environment&agencyName=Air%20Quality%20Control%20Commission&seriesNum=5%20CCR%201001-9>.
- (12) Brandt, A.R.; Heath, G.A.; Cooley, D. Methane Leaks from Natural Gas Systems Follow Extreme Distributions. *Environmental Science & Technology*, **2016**, 50(22), pp.12512–12520. DOI: 10.1021/acs.est.6b04303.
- (13) Scarpelli, T.R.; Jacob, D.J.; Grossman, S.; Lu, X.; Qu, Z.; Sulprizio, M.P.; Zhang, Y.; Reuland, F.; Gordon, D.; Worden, J.R. Updated Global Fuel Exploitation Inventory (GFEI) for methane emissions from the oil, gas, and coal sectors: evaluation with inversions of atmospheric methane observations. *Atmospheric Chemistry and Physics*, **2022**, 22(5), pp.3235–3249. DOI: 10.5194/acp-22-3235-2022.
- (14) Vaughn, T.L.; Bell, C.S.; Pickering, C.K.; Schwietzke, S.; Heath, G.A.; Pétron, G.; Zimmerle, D.J.; Schnell, R.C.; Nummedal, D. Temporal variability largely explains top-down/bottom-up difference in methane emission estimates from a natural gas production region. *Proceedings of the National Academy of Sciences*, **2018**, 115(46), pp.11712–11717. DOI: 10.1073/pnas.1805687115.
- (15) Daniels, W.S.; Wang, J.L.; Ravikumar, A.P.; Harrison, M.; Roman-White, S.A.; George, F.C.; Hammerling, D.M. Toward Multiscale Measurement-Informed Methane Inventories: Reconciling Bottom-Up Site-Level Inventories with Top-Down Measurements Using Continuous Monitoring Systems. *Environmental Science & Technology* **2023**, 57(32), pp.11823–11833. DOI: 10.1021/acs.est.3c01121.

- (16) Johnson, M.R.; Conrad, B.M.; Tyner, D.R. Creating measurement-based oil and gas sector methane inventories using source-resolved aerial surveys. *Communications Earth & Environment* **2023**, *4*(1). DOI: 10.1038/s43247-023-00769-7.
- (17) Conrad, B.M.; Tyner, D.R.; Johnson, M.R. The Futility of Relative Methane Reduction Targets in the Absence of Measurement-Based Inventories. *Environmental Science & Technology* **2023**, *57*(50), pp.21092–21103. DOI: 10.1021/acs.est.3c07722.
- (18) MacKay, K.; Seymour, S.P.; Li, H.Z.; Zavala-Araiza, D.; Xie, D. A Comprehensive Integration and Synthesis of Methane Emissions from Canada's Oil and Gas Value Chain. *Environmental Science & Technology* **2024**, *58*(32), pp.14203–14213. DOI: 10.1021/acs.est.4c03651.
- (19) Riddick, S.N.; Mbua, M.; Anand, A.; Kiplimo, E.; Santos, A.; Upreti, A.; Zimmerle, D.J. Estimating Total Methane Emissions from the Denver-Julesburg Basin Using Bottom-Up Approaches. *Gases* **2024**, *4*(3), pp.236–252. DOI: 10.3390/gases4030014.
- (20) Rutherford, J.S.; Sherwin, E.D.; Ravikumar, A.P.; Heath, G.A.; Englander, J.; Cooley, D.; Lyon, D.; Omara, M.; Langfitt, Q.; Brandt, A.R. Closing the methane gap in US oil and natural gas production emissions inventories. *Nature Communications* **2021**, *12*(1). DOI: 10.1038/s41467-021-25017-4.
- (21) Scarpelli, T.R.; Jacob, D.J.; Grossman, S.; Lu, X.; Qu, Z.; Sulprizio, M.P.; Zhang, Y.; Reuland, F.; Gordon, D.; Worden, J.R. Updated Global Fuel Exploitation Inventory (GFEI) for methane emissions from the oil, gas, and coal sectors: evaluation with inversions of atmospheric methane observations. *Atmospheric Chemistry and Physics* **2022**, *22*(5), pp.3235–3249. DOI: 10.5194/acp-22-3235-2022.
- (22) Wang, J.L.; Daniels, W.S.; Hammerling, D.M.; Harrison, M.; Burmaster, K.; George, F.C.; Ravikumar, A.P. Multiscale Methane Measurements at Oil and Gas Facilities Reveal Necessary Frameworks for Improved Emissions Accounting. *Environmental Science & Technology* **2022**, *56*(20), pp.14743–14752. DOI: 10.1021/acs.est.2c06211.
- (23) Carl, R.; Mike, B.; George, P.; John, D. OGC® Sensor Web Enablement: Overview And High Level Architecture. *OGC.org* **2013**. DOI: 07-165r1.
- (24) ISO. ISO 19156:2023. *International Organization for Standardization* **2023**. Available at: <https://www.iso.org/standard/82463.html#lifecycle> (accessed 12 Jun 2025).
- (25) Fox, T.A.; Barchyn, T.E.; Risk, D.; Ravikumar, A.P.; Hugenholtz, C.H. A review of close-range and screening technologies for mitigating fugitive methane emissions in upstream oil and gas. *Environmental Research Letters* **2019**, *14*(5), 053002. DOI: 10.1088/1748-9326/ab0cc3.
- (26) Anselin, L. Local Indicators of Spatial Association—LISA. *Geographical Analysis* **1995**, *27*(2), pp.93–115. DOI: 10.1111/j.1538-4632.1995.tb00338.x.
- (27) Allen, J.F. Maintaining knowledge about temporal intervals. *Communications of the ACM* **1983**, *26*(11), pp.832–843. DOI: 10.1145/182.358434.
- (28) US EPA. 40 CFR Part 98 Subpart W—Petroleum and Natural Gas Systems. *Code of Federal Regulations* **2025**. Available at: <https://www.ecfr.gov/current/title-40/chapter-I/subchapter-C/part-98/subpart-W>.
- (29) Higgins, S.; Hecobian, A.; Baasandorj, M.; Pacsi, A.P. A Practical Framework for Oil and Gas Operators to Estimate Methane Emission Duration Using Operational Data. *SPE Journal* **2024**, *29*(5). DOI: 10.2118/219445-pa.
- (30) Bell, C.S.; Ilonze, C.; Duggan, A.; Yuan, S. Performance of Continuous Emission Monitoring Solutions under a Single-Blind Controlled Testing Protocol. *Environmental Science & Technology* **2023**, *57*, pp.5794–5805. DOI: 10.1021/acs.est.2c09235.

- (31) Daniels, W.S.; Jia, M.; Hammerling, D.M. Estimating Methane Emission Durations Using Continuous Monitoring Systems. *Environmental Science & Technology Letters* **2024**, *11*(11), pp.1187–1192. DOI: 10.1021/acs.estlett.4c00687.
- (32) Government of Canada. Regulations Respecting Reduction in the Release of Methane and Certain Volatile Organic Compounds (Upstream Oil and Gas Sector) (SOR/2018-66). *Justice Laws Website* **2025**. Available at: <https://laws-lois.justice.gc.ca/eng/regulations/SOR-2018-66/> (accessed 13 Jun 2025).
- (33) Fox, T.A.; Gao, M.; Barchyn, T.E.; Jamin, Y.L.; Hugenholtz, C.H. An agent-based model for estimating emissions reduction equivalence among leak detection and repair programs. *Journal of Cleaner Production* **2021**, *282*, 125237. DOI: 10.1016/j.jclepro.2020.125237.
- (34) Kemp, C.E.; Ravikumar, A.P.; Brandt, A.R. Comparing Natural Gas Leakage Detection Technologies Using an Open-Source ‘Virtual Gas Field’ Simulator. *Environmental Science & Technology* **2016**, *50*(8), pp.4546–4553. DOI: 10.1021/acs.est.5b06068.
- (35) Koehler, E.; Brown, E.; Haneuse, S.J.-P.A. On the Assessment of Monte Carlo Error in Simulation-Based Statistical Analyses. *The American Statistician* **2009**, *63*(2), pp.155–162. DOI: 10.1198/tast.2009.0030.
- (36) IPCC. IPCC - Task Force on National Greenhouse Gas Inventories. *IGES* **2019**. Available at: <https://www.ipcc-nggip.iges.or.jp/public/2006gl/>.
- (37) Conrad, B.M.; Tyner, D.R.; Johnson, M.R. Robust probabilities of detection and quantification uncertainty for aerial methane detection: Examples for three airborne technologies. *Remote Sensing of Environment* **2023**, *288*, 113499. DOI: 10.1016/j.rse.2023.113499.
- (38) Hersbach, H.; Bell, B.; Berrisford, P.; Biavati, G.; Horányi, A.; Muñoz Sabater, J.; Nicolas, J.; Peubey, C.; Radu, R.; Rozum, I.; Schepers, D.; Simmons, A.; Soci, C.; Dee, D.; Thépaut, J.-N. ERA5 hourly data on single levels from 1940 to present. *Copernicus Climate Change Service (C3S) Climate Data Store (CDS)* **2023**. DOI: 10.24381/cds.adbb2d47.
- (39) MiQ. *Monitoring Technology Compatibility Assessment Qube Axon*. 2024. <https://miq.org/document/qube-compatibility-assessment-2>.
- (40) Open Geospatial Consortium. *OGC to Form Emission Event Modeling Language Working Group: Public Comment Sought on Charter*. 2024. <https://www.ogc.org/requests/ogc-to-form-emission-event-modeling-language-working-group-public-comment-sought-on-charter/>

Supporting Information for:

An Event-Based Framework for Estimating Annual Methane Emissions and Managing Emissions Data from Upstream Oil and Gas Facilities

Mozhou Gao^{1,4}, Zahra Ashena^{1,3}, Steve H.L. Liang^{1,3}, Sina Kiaei^{1,3}, and Sara Saeedi^{1,2}

¹GeoSensorWeb Lab, Department of Geomatics Engineering, Schulich School of Engineering, University of Calgary, 2500 University Dr. NW, Calgary, AB, Canada

²Department of Electrical and Software Engineering, Schulich School of Engineering, University of Calgary, 2500 University Dr. NW, Calgary, AB, Canada

³SensorUp Inc., Calgary, AB, Canada

⁴Kuruktag Emissions Ltd., Coquitlam, BC, Canada

Email: mozhou.gao@ucalgary.ca

Table of Contents

S1. Emissions event data model (EEDM) and Allen's time algebra	32
S2. Synthetic emissions observations.....	34
S3. Results for case study No.1	39
S4. Results for case study No.2	42

S1. Emissions event data model (EEDM) and Allen's time algebra

The UML definition of the emissions event data model (EEDM) can be expressed as follows:

```
class EmissionsEvent {  
  - eventType: enumeration  
  - hasDuration: Duration  
  - hasCause: Cause  
  - hasSource: Source  
  - hasQuantity: Quantity  
  - hasObservation: Observation[*]  
}  
  
class Duration {  
  + value: float  
  + unit: string  
}  
  
class Cause {  
  + causeType: string  
}  
  
class Source {  
  + geometry: feature  
  + sourceCategory: enumeration  
  + equipment: enumeration  
}  
  
class Quantity {  
  + value: float  
  + unit: string  
  - isCalculatedBy: Observation  
  - isDeterminedBy: ObservationF  
}  
  
class Observation {  
  + value: float  
  + unit: string  
  + observationType: enumeration  
  + observationTime: datetime  
  + startTime: datetime  
  + endTime: datetime  
}  
  
class EventGrouping {  
  - spatialProximity: boolean  
  - temporalRelationship: enumeration  
  - groups: EmissionsEvent[*]  
}
```

Where *Observation*[*] in EE allows multiple emissions observations (EOs) to be associated with a single EE. *EventGrouping* class is not included in the Figure 1 of main paper. It represents the logic of grouping EOs using spatial proximity and Allen's interval algebra. The *groups* tracks merged emission events.

To group EOs into a single EE or merge multiple EEs into one EE, the model uses spatial proximity to indicate if observations are geographically close or directly/indirectly attributed to the same physical emission sources (equipment). The *temporalRelationship* indicates the temporal relations between EOs or EEs based on Allen’s Interval Algebra (Allen, 1983).

Table S1: Illustration of Allen’s interval algebra logic between two-time intervals.

Relation	Illustration
T1 precedes T2	T1
T2 precededBy T1	T2
T1 meets T2	T1
T2 metBy T1	T2
T1 overlaps T2	T1
T2 overlappedBy T1	T2
T1 starts T2	T1
T2 startedBy T1	T2
T1 during T2	T1
T2 contains T1	T2
T1 finishes T2	T1
T2 finishedBy T1	T2
T1 equals T2	T1
	T2

As illustrated in Table S1, thirteen fundamental temporal relationships are defined: *precedes*, *preceded by*, *meets*, *met by*, *overlaps*, *overlapped by*, *contains*, *during*, *starts*, *started by*, *finishes*, *finished by*, and *equals* [1]. Except for *precedes* and *preceded by*, if two or more EOs or EEs satisfy any of the other eleven relationships and are also spatially close (or attributed to the same equipment), they are more likely to originate from the same emission within the same emission event. For example, we can conclude that the CMS alarm and VFB can be correlated as the same event, when a CMS alarm indicating emissions from Compressor A between 2024-07-05T09:00:00 and 2024-07-05T11:00:00 *contains* Compressor rod packing venting reported for Compressor A from 2024-07-05T10:20:00 to 2024-07-05T10:50:00.

EEDM uses a network of nodes and edges to identify temporal rules based on relationships between emission observations within the same event. Each observation is a node within an event, while edges represent the spatiotemporal correlations between them. The observation with the earliest timestamp is defined as the parent, and all other observations are considered child observations. When two events merge, child and parent observations are redefined accordingly.

The parent observation plays a crucial role in PREs that contain only instantaneous measurement observations, particularly when duration must be inferred from preceding and succeeding null detections.

S2. Synthetic emissions observations

Table S2. Synthetic emissions observations in the case study No.1.

ID	site	equipment	start time	end time	rate (kg/hr)
CMS-89	A	Compressor-3	01-01-2024 2:16	01-01-2024 18:46	13.43743062
CMS-88	A	Compressor-2	01-01-2024 17:12	02-01-2024 0:32	11.0537834
CMS-87	A	Dehydrator-1	02-01-2024 8:38	03-01-2024 2:14	6.485984945
CMS-86	A	Dehydrator-1	03-01-2024 1:20	03-01-2024 17:55	9.745295575
CMS-85	A	Dehydrator-1	03-01-2024 23:33	04-01-2024 3:06	5.279977194
CMS-84	A	Dehydrator-1	04-01-2024 12:02	04-01-2024 20:25	44.44340994
CMS-83	A	Dehydrator-1	05-01-2024 12:21	05-01-2024 14:09	26.4754512
CMS-82	A	Dehydrator-1	05-01-2024 18:40	06-01-2024 15:03	10.2931667
CMS-81	A	Dehydrator-1	06-01-2024 12:55	07-01-2024 6:39	22.90488356
CMS-80	A	Dehydrator-1	07-01-2024 3:28	07-01-2024 7:34	4.38235222
CMS-79	A	Dehydrator-1	07-01-2024 15:50	08-01-2024 5:10	15.68792648
CMS-78	A	Dehydrator-1	08-01-2024 21:11	09-01-2024 5:36	23.01335768
CMS-77	A	Dehydrator-1	09-01-2024 4:54	09-01-2024 15:33	16.46214129
CMS-76	A	Dehydrator-1	09-01-2024 20:05	10-01-2024 10:21	6.575924082
CMS-75	A	Dehydrator-1	10-01-2024 9:17	11-01-2024 20:43	9.97428315
CMS-74	A	Dehydrator-1	12-01-2024 8:57	15-01-2024 9:31	39.60280338
CMS-73	A	Dehydrator-1	15-01-2024 9:19	15-01-2024 12:30	4.631917288
CMS-72	A	Compressor-2	15-01-2024 11:46	16-01-2024 6:06	127.1398731
CMS-71	A	Compressor-3	16-01-2024 11:53	17-01-2024 3:15	50.81348771
CMS-70	A	Compressor-2	17-01-2024 10:29	19-01-2024 23:15	9.865365612
CMS-69	A	Tank-2	20-01-2024 17:49	21-01-2024 0:07	7.830741333
CMS-68	A	Compressor-2	21-01-2024 7:16	22-01-2024 0:02	7.280364451
CMS-67	A	Compressor-3	22-01-2024 2:24	22-01-2024 7:15	1.872333732
CMS-66	A	Compressor-3	22-01-2024 6:48	23-01-2024 1:56	11.11957246
CMS-65	A	Tank-1	22-01-2024 13:05	23-01-2024 2:59	15.78909064
CMS-63	A	Dehydrator-1	23-01-2024 16:02	24-01-2024 8:27	19.49150927
CMS-64	A	Dehydrator-1	23-01-2024 16:02	24-01-2024 6:27	27.31177958
CMS-62	A	Dehydrator-1	24-01-2024 15:06	25-01-2024 1:46	17.92923359
CMS-61	A	Dehydrator-1	25-01-2024 16:45	26-01-2024 5:08	19.41097409
CMS-60	A	Dehydrator-1	26-01-2024 13:50	27-01-2024 6:36	22.35054016
CMS-59	A	Dehydrator-1	27-01-2024 1:45	27-01-2024 8:08	13.98306741
CMS-57	A	Dehydrator-1	27-01-2024 10:10	28-01-2024 3:15	13.09969511
CMS-58	A	Dehydrator-1	27-01-2024 10:10	27-01-2024 23:37	16.04159662
CMS-56	A	Dehydrator-1	28-01-2024 15:43	28-01-2024 23:59	10.05147194
CMS-55	A	Dehydrator-1	29-01-2024 15:48	30-01-2024 0:36	12.67874941

CMS-54	A	Dehydrator-1	31-01-2024 17:15	01-02-2024 3:30	60.47970498
CMS-53	A	Dehydrator-1	01-02-2024 13:45	01-02-2024 22:38	10.77638599
CMS-52	A	Dehydrator-1	02-02-2024 23:30	03-02-2024 6:10	24.7853662
CMS-51	A	Dehydrator-1	03-02-2024 11:03	03-02-2024 15:53	17.19845255
CMS-50	A	Dehydrator-1	04-02-2024 13:38	05-02-2024 8:05	23.45762222
CMS-49	A	Dehydrator-1	07-02-2024 4:05	07-02-2024 9:11	14.86192301
CMS-48	A	Dehydrator-1	07-02-2024 17:09	07-02-2024 21:40	13.72649872
CMS-47	A	Dehydrator-1	08-02-2024 8:39	08-02-2024 14:27	17.22924512
CMS-45	A	Dehydrator-1	08-02-2024 17:30	09-02-2024 4:10	11.86600299
CMS-46	A	Dehydrator-1	08-02-2024 17:30	09-02-2024 4:10	14.76924197
CMS-44	A	Dehydrator-1	10-02-2024 6:47	10-02-2024 16:31	6.821435342
CMS-43	A	Dehydrator-1	10-02-2024 14:50	10-02-2024 23:17	28.89126158
CMS-42	A	Dehydrator-1	11-02-2024 15:45	12-02-2024 5:38	123.3328614
CMS-41	A	Dehydrator-1	16-02-2024 11:51	16-02-2024 16:46	14.83360889
CMS-40	A	Dehydrator-1	22-02-2024 2:22	22-02-2024 9:08	17.60689626
CMS-39	A	Dehydrator-1	22-02-2024 11:25	23-02-2024 4:36	33.41612275
CMS-38	A	Compressor-2	23-02-2024 14:04	24-02-2024 3:23	18.51180616
CMS-37	A	Compressor-2	24-02-2024 8:34	24-02-2024 18:34	11.69312178
CMS-36	A	Compressor-2	27-02-2024 10:58	27-02-2024 15:44	14.44655555
CMS-35	A	Compressor-2	01-03-2024 17:52	01-03-2024 23:27	16.77220239
CMS-34	A	Compressor-2	03-03-2024 4:38	03-03-2024 22:15	17.15981442
CMS-33	A	Compressor-3	07-03-2024 5:57	07-03-2024 10:56	11.42898031
CMS-32	A	Compressor-2	07-03-2024 7:16	07-03-2024 15:02	16.23481555
CMS-31	A	Compressor-2	08-03-2024 12:23	10-03-2024 0:18	14.71608663
CMS-29	A	Compressor-3	14-03-2024 9:15	14-03-2024 23:52	15.29498708
CMS-30	A	Tank-1	14-03-2024 9:15	14-03-2024 23:52	14.74954203
CMS-28	A	Tank-1	15-03-2024 7:54	15-03-2024 19:43	10.83058592
CMS-27	A	Compressor-2	18-03-2024 15:35	19-03-2024 1:32	13.08735161
CMS-25	A	Separator-2	21-03-2024 16:45	22-03-2024 2:54	12.4923744
CMS-26	A	Dehydrator-2	21-03-2024 16:45	22-03-2024 2:54	15.49997366
CMS-24	A	Separator-2	22-03-2024 11:45	23-03-2024 4:40	19.45596602
CMS-23	A	Separator-2	23-03-2024 15:56	24-03-2024 8:16	20.77621499
CMS-22	A	Separator-2	29-03-2024 12:10	29-03-2024 18:10	50.5477992
CMS-21	A	Separator-2	05-04-2024 14:08	05-04-2024 17:58	19.2303107
CMS-20	A	Separator-2	05-04-2024 15:40	05-04-2024 20:41	53.27457756
CMS-19	A	Separator-2	06-04-2024 1:59	06-04-2024 5:50	18.95548269
CMS-18	A	Separator-2	09-04-2024 8:27	09-04-2024 19:36	18.53332709
CMS-17	A	Separator-2	10-04-2024 14:25	11-04-2024 0:11	140.6241274
CMS-16	A	Separator-2	11-04-2024 15:06	11-04-2024 22:43	55.89072104
CMS-15	A	Separator-2	12-04-2024 14:09	12-04-2024 22:15	29.79022037
CMS-14	A	Separator-1	13-04-2024 0:00	13-04-2024 8:05	14.72482916
CMS-13	A	Separator-1	14-04-2024 1:54	14-04-2024 5:54	16.01493411
CMS-11	A	Separator-1	16-04-2024 4:25	16-04-2024 10:40	13.04163146

CMS-12	A	Separator-1	16-04-2024 4:25	16-04-2024 10:40	9.677583744
CMS-10	A	Separator-1	17-04-2024 5:04	17-04-2024 14:09	24.53500301
CMS-9	A	Separator-1	18-04-2024 13:26	18-04-2024 20:51	14.93944563
CMS-8	A	Separator-1	18-04-2024 22:32	19-04-2024 2:41	17.65106764
CMS-7	A	Separator-1	19-04-2024 14:49	20-04-2024 2:49	35.81272269
CMS-6	A	Separator-2	20-04-2024 14:10	20-04-2024 16:35	77.00366334
CMS-5	A	Separator-1	22-04-2024 14:00	23-04-2024 10:07	77.63196097
CMS-4	A	Separator-1	26-04-2024 10:15	26-04-2024 16:38	10.80466042
CMS-3	A	Separator-1	27-04-2024 6:05	27-04-2024 13:57	16.03540446
CMS-2	A	Separator-1	28-04-2024 7:12	28-04-2024 19:16	11.16171355
CMS-1	A	Separator-1	29-04-2024 23:25	30-04-2024 4:48	29.86309642

Table S3. Synthetic flyover measurements in the case study No.1.

ID	site	equipment	detection time	detection	survey time	rate (kg/hr)
FLY-1	A			FALSE	07-01-2024 17:31	1538.3
FLY-2	A	Compressor-2	22-02-2024 19:40	TRUE	22-02-2024 15:40	53
FLY-3	A	Compressor-3	22-03-2024 19:40	TRUE	22-03-2024 16:40	64
FLY-4	A		05-04-2024 19:14	TRUE	05-04-2024 16:14	38.5

Table S4. Synthetic OGI measurements in the case study No.1.

ID	site	equipment	detection	survey time	number of leaks
OGI-1	A		FALSE	01-01-2024 17:31	0
OGI-2	A	Compressor-2	TRUE	01-02-2024 15:40	2
OGI-3	A	Separator-2	TRUE	01-03-2024 16:40	4
OGI-4	A		FALSE	01-04-2024 16:14	0

Table S5. Synthetic venting events in the case study No.1.

ID	site	equipment	start time	end time	total emissions (kg)
OP-1	A	Compressor-3	01-01-2024 4:25	01-01-2024 4:35	182.79626
OP-2	A	Tank-1	01-01-2024 13:34	01-01-2024 13:40	231.25869
OP-3	A	Tank-1	02-01-2024 6:50	02-01-2024 6:57	159.22217
OP-4	A	Tank-1	03-01-2024 15:15	03-01-2024 15:20	263.07187
OP-5	A	Compressor-2	05-01-2024 7:30	05-01-2024 7:35	339.0873
OP-6	A	Tank-2	06-01-2024 0:40	06-01-2024 0:50	263.41729
OP-7	A	Compressor-3	06-01-2024 11:30	06-01-2024 11:35	263.41729
OP-8	A	Compressor-3	06-01-2024 17:25	06-01-2024 17:30	333.67572
OP-9	A	Compressor-2	07-01-2024 1:30	07-01-2024 1:35	537.58866
OP-10	A	Compressor-2	07-01-2024 9:30	07-01-2024 9:35	3515.5696
OP-11	A	Compressor-2	07-01-2024 11:00	07-01-2024 11:05	335.88641

OP-12	A	Compressor-3	08-01-2024 9:35	08-01-2024 9:40	311.91426
OP-13	A	Compressor-2	10-01-2024 7:30	10-01-2024 7:35	390.3246
OP-14	A	Compressor-2	10-01-2024 9:50	10-01-2024 9:55	401.44712
OP-15	A	Tank-1	12-01-2024 9:45	12-01-2024 10:35	606.50225
OP-16	A	Compressor-3	23-01-2024 7:10	23-01-2024 7:15	416.32321
OP-17	A	Tank-1	25-01-2024 9:00	25-01-2024 10:00	432.74218
OP-18	A	Compressor-2	03-02-2024 7:40	03-02-2024 7:45	339.84722
OP-19	A	Dehydrator-2	05-02-2024 14:14	16-02-2024 11:45	2.0650047
OP-20	A	Compressor-2	10-02-2024 8:41	10-02-2024 8:45	307.9995
OP-21	A	Compressor-3	10-02-2024 9:04	10-02-2024 9:07	480.05704
OP-22	A	Compressor-2	10-02-2024 10:14	10-02-2024 10:16	541.158
OP-23	A	Compressor-2	10-02-2024 11:00	10-02-2024 11:03	423.1395
OP-24	A	Compressor-2	13-02-2024 8:30	13-02-2024 9:10	382.33676
OP-25	A	Compressor-1	25-02-2024 7:22	25-02-2024 7:24	413.12232
OP-26	A	Compressor-1	26-02-2024 14:35	26-02-2024 14:37	615.999
OP-27	A	Compressor-3	29-02-2024 17:20	29-02-2024 17:25	309.03576
OP-28	A	Compressor-1	01-03-2024 11:45	01-03-2024 11:50	278.43155
OP-29	A	Compressor-1	16-03-2024 11:10	16-03-2024 11:15	347.5616
OP-30	A	Compressor-2	18-03-2024 9:10	18-03-2024 9:15	212.77872
OP-31	A	Compressor-1	20-03-2024 14:45	20-03-2024 14:47	513.98496
OP-32	A	Compressor-3	02-04-2024 10:23	02-04-2024 10:26	454.11216
OP-33	A	Compressor-1	06-04-2024 9:20	06-04-2024 9:26	245.70876
OP-34	A	Compressor-3	20-04-2024 13:19	20-04-2024 13:24	288.05024
OP-35	A	Compressor-3	22-04-2024 3:03	22-04-2024 3:14	123.09513
OP-36	A	Compressor-3	22-04-2024 6:40	22-04-2024 6:45	320.91821
OP-37	A	Compressor-1	23-04-2024 8:20	23-04-2024 8:25	415.77054
OP-38	A	Compressor-3	23-04-2024 11:40	23-04-2024 11:45	385.90322
OP-39	A	Compressor-2	26-04-2024 0:12	26-04-2024 0:35	53.88552
OP-40	A	Compressor-1	26-04-2024 22:20	26-04-2024 22:30	119.37715
OP-41	A	Compressor-2	27-04-2024 8:24	27-04-2024 8:35	147.85023
OP-42	A	Tank-3	27-04-2024 15:08	27-04-2024 15:24	122.45859
OP-43	A	Compressor-1	29-04-2024 23:13	29-04-2024 23:20	176.32869
OP-44	A	Compressor-2	29-04-2024 23:20	29-04-2024 23:26	229.5124
OP-45	A	Compressor-3	30-04-2024 2:05	30-04-2024 2:13	266.69303
OP-46	A	Compressor-2	30-04-2024 4:10	30-04-2024 4:19	221.6445
OP-47	A	Tank-2	30-04-2024 6:37	30-04-2024 6:50	1152.1794
OP-48	A	Compressor-2	30-04-2024 8:12	30-04-2024 8:23	109.69702
OP-49	A	Compressor-3	30-04-2024 9:50	30-04-2024 9:58	182.61204

Table S6. Synthetic CMS measurement in the case study No.2.

ID	site	equipment	start time	end time	rate (kg/hr)
CMS-1	B	Compressor-3	01-01-2024 2:16	01-01-2024 18:46	13.43743062
CMS-2	B	Compressor-2	01-01-2024 17:12	02-01-2024 0:32	11.0537834
CMS-3	B	Tank-1	02-01-2024 8:38	03-01-2024 2:14	6.485984945
CMS-4	B	Dehydrator-1	03-01-2024 1:20	03-01-2024 17:55	9.745295575
CMS-5	B	Tank-1	03-01-2024 23:33	04-01-2024 3:06	5.279977194
CMS-6	B	Separator-1	04-01-2024 12:02	04-01-2024 20:25	44.44340994
CMS-7	B	Dehydrator-1	05-01-2024 12:21	05-01-2024 14:09	26.4754512
CMS-8	B	Separator-2	05-01-2024 18:40	06-01-2024 15:03	10.2931667
CMS-9	B	Dehydrator-1	06-01-2024 12:55	07-01-2024 6:39	22.90488356
CMS-10	B	Separator-3	07-01-2024 3:28	07-01-2024 7:34	4.38235222
CMS-11	B	Tank-1	07-01-2024 15:50	08-01-2024 5:10	15.68792648
CMS-12	B	Dehydrator-1	08-01-2024 21:11	09-01-2024 5:36	23.01335768
CMS-13	B	Dehydrator-1	09-01-2024 4:54	09-01-2024 15:33	16.46214129
CMS-14	B	Dehydrator-1	09-01-2024 20:05	10-01-2024 10:21	6.575924082
CMS-15	B	Dehydrator-1	10-01-2024 9:17	11-01-2024 20:43	9.97428315
CMS-16	B	Tank-1	12-01-2024 8:57	15-01-2024 9:31	39.60280338
CMS-17	B	Dehydrator-1	15-01-2024 9:19	15-01-2024 12:30	4.631917288
CMS-18	B	Compressor-2	15-01-2024 11:46	16-01-2024 6:06	127.1398731
CMS-19	B	Compressor-3	16-01-2024 11:53	17-01-2024 3:15	50.81348771
CMS-20	B	Compressor-2	17-01-2024 10:29	19-01-2024 23:15	9.865365612
CMS-21	B	Tank-2	20-01-2024 17:49	21-01-2024 0:07	7.830741333
CMS-22	B	Compressor-2	21-01-2024 7:16	22-01-2024 0:02	7.280364451
CMS-23	B	Compressor-3	22-01-2024 2:24	22-01-2024 7:15	1.872333732
CMS-24	B	Wellhead	22-01-2024 6:48	23-01-2024 1:56	11.11957246
CMS-25	B	Tank-1	22-01-2024 13:05	23-01-2024 2:59	15.78909064
CMS-26	B	Dehydrator-1	23-01-2024 16:02	24-01-2024 8:27	19.49150927
CMS-27	B	Compressor-1	23-01-2024 16:02	24-01-2024 6:27	27.31177958
CMS-28	B	Dehydrator-1	24-01-2024 15:06	25-01-2024 1:46	17.92923359
CMS-29	B	Separator-2	25-01-2024 16:45	26-01-2024 5:08	19.41097409
CMS-30	B	Dehydrator-1	26-01-2024 13:50	27-01-2024 6:36	22.35054016
CMS-31	B	Dehydrator-1	27-01-2024 1:45	27-01-2024 8:08	13.98306741
CMS-32	B	Separator-2	27-01-2024 10:10	28-01-2024 3:15	13.09969511
CMS-33	B	Compressor-1	27-01-2024 10:10	27-01-2024 23:37	16.04159662
CMS-34	B	Separator-2	28-01-2024 15:43	28-01-2024 23:59	10.05147194
CMS-35	B	Dehydrator-1	29-01-2024 15:48	30-01-2024 0:36	12.67874941
CMS-36	B	Tank-2	31-01-2024 17:15	01-02-2024 3:30	60.47

S3. Results for case study No.1

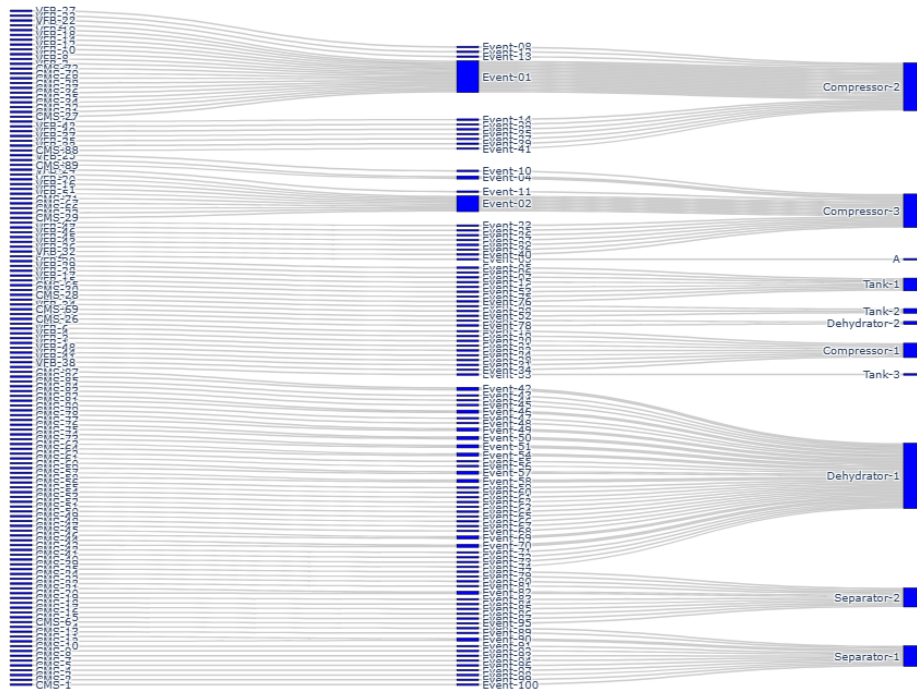


Figure S1. Sankey diagram describing how EOs are merged to EEs and are attributed to equipment in case study No.1.

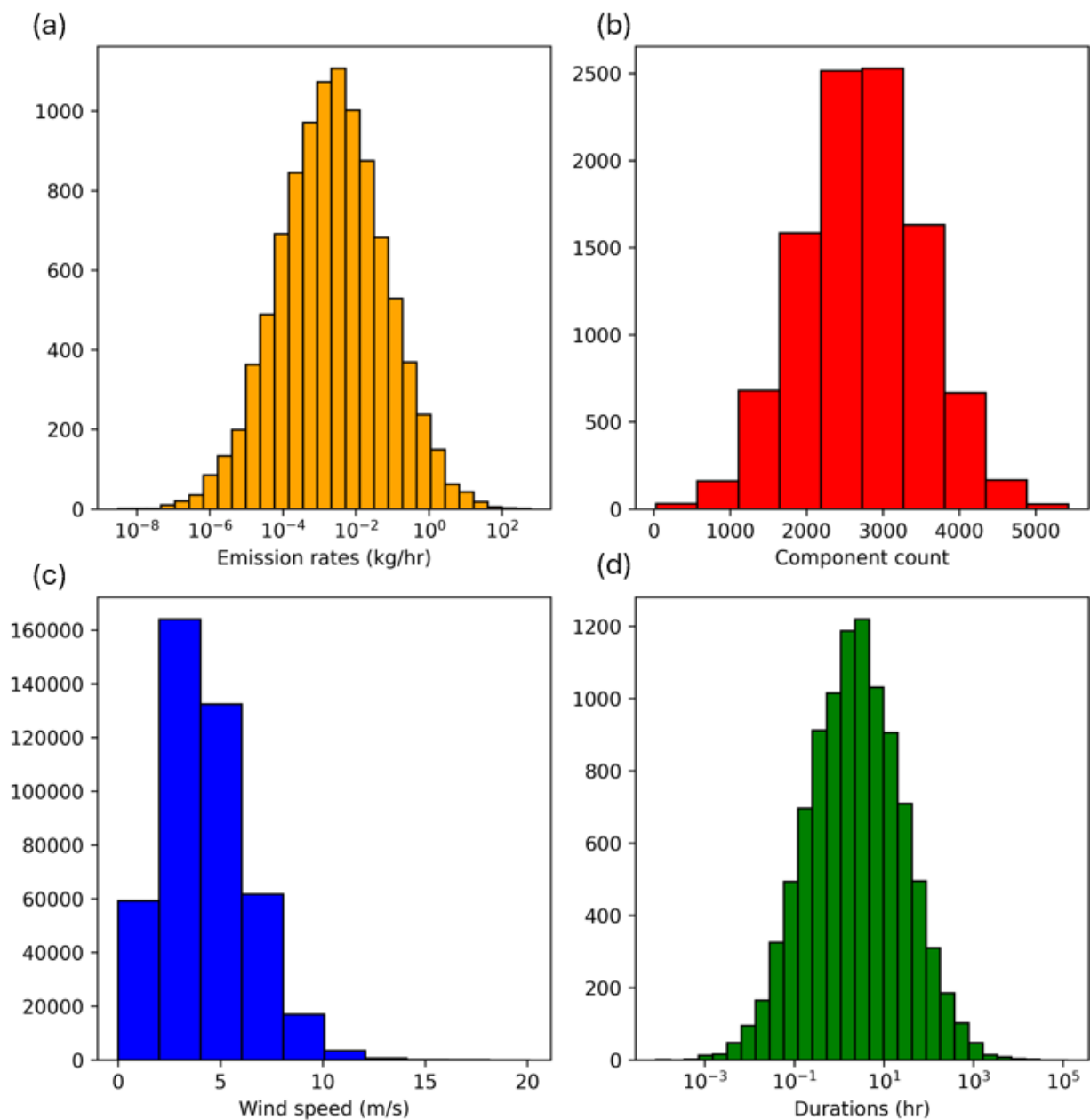


Figure S2. Inputs for simulating emissions from unresolved events that are below the minimum detection limit of deployed technologies. (a). component-scale emissions rate (Rutherford et al., 2021); (b) Component count used for scaling component-scale emissions to equipment-scale emissions; (c) Wind speed data downloaded from ERA5; (d) event durations from all REs and PREs.

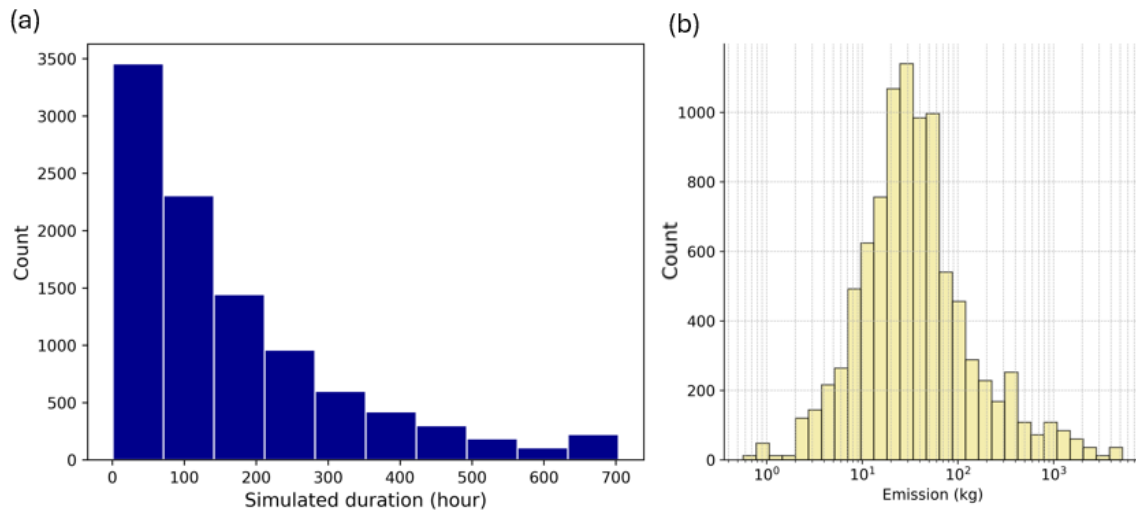


Figure S3. Simulation results from 10,000 Monte Carlo runs. (a) Duration simulation results using preceding and succeeding non-detects derived from the OGI survey. (b) Simulated emission quantities from unresolved events under the scenarios defined in Case Study No. 1.

S4. Results for case study No.2

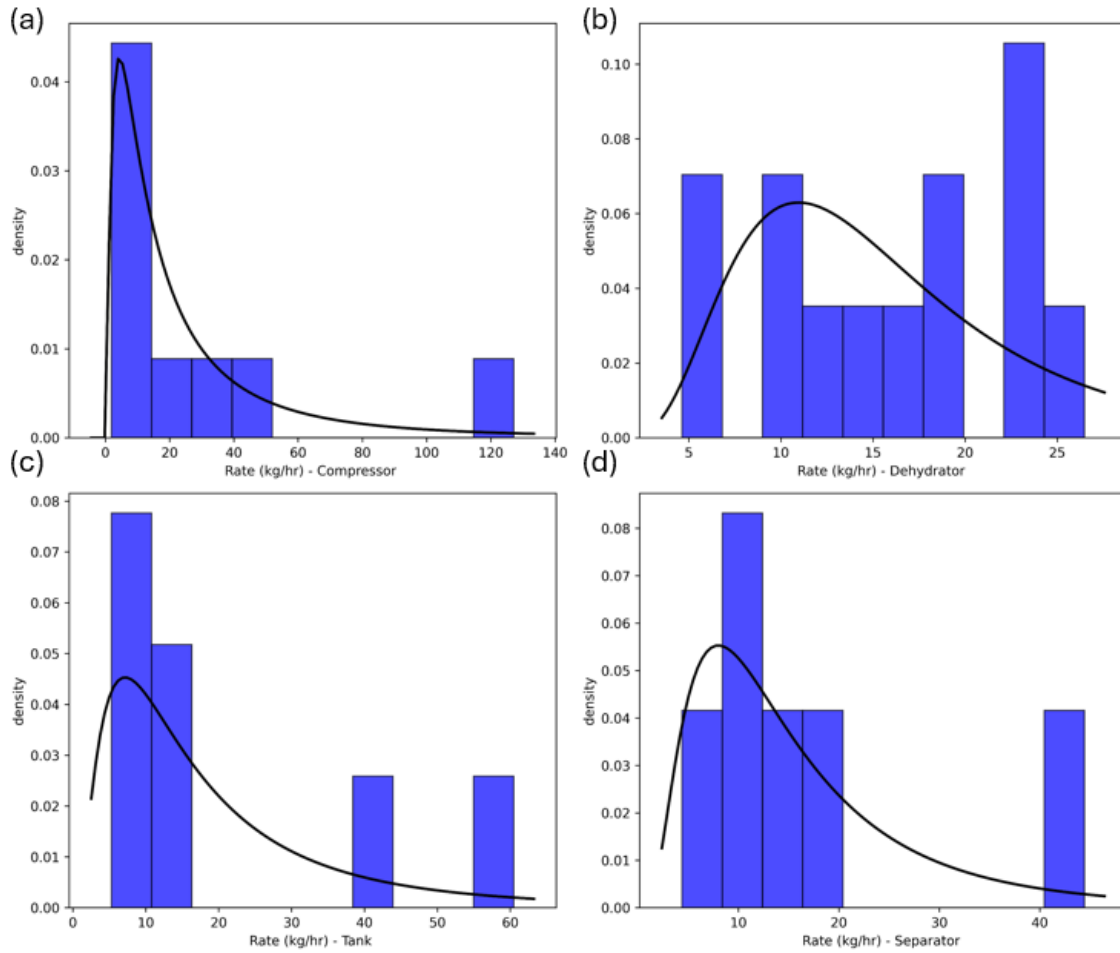


Figure S4. Best-fitted rate curves based on rates from all PREs by equipment type: (a) compressors, (b) dyhydrators, (c) tanks and (d) separators.

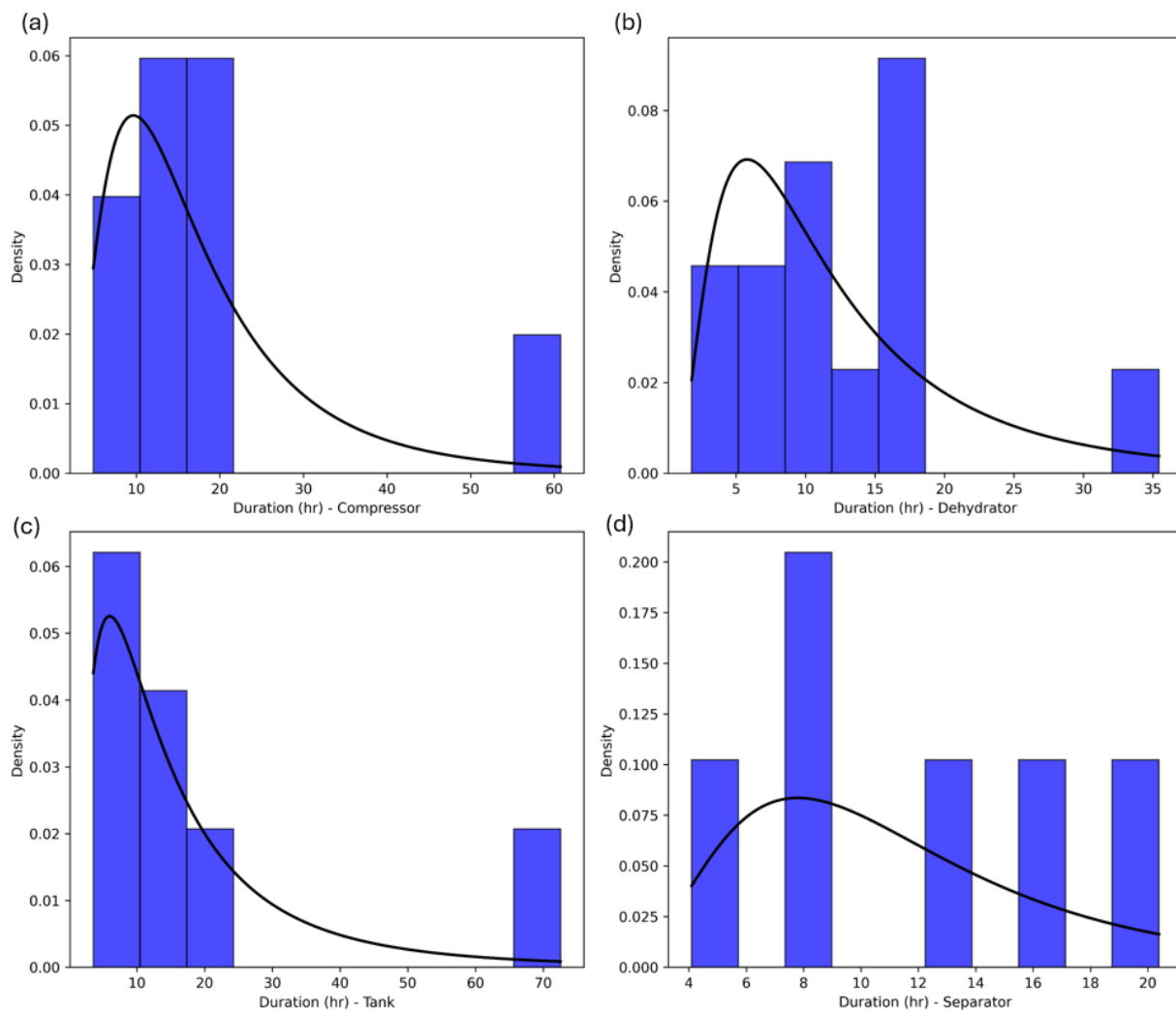


Figure S5. Best-fitted duration curves based on durations from all PREs by equipment type: (a) compressors, (b) dehydrators, (c) tanks and (d) separators.

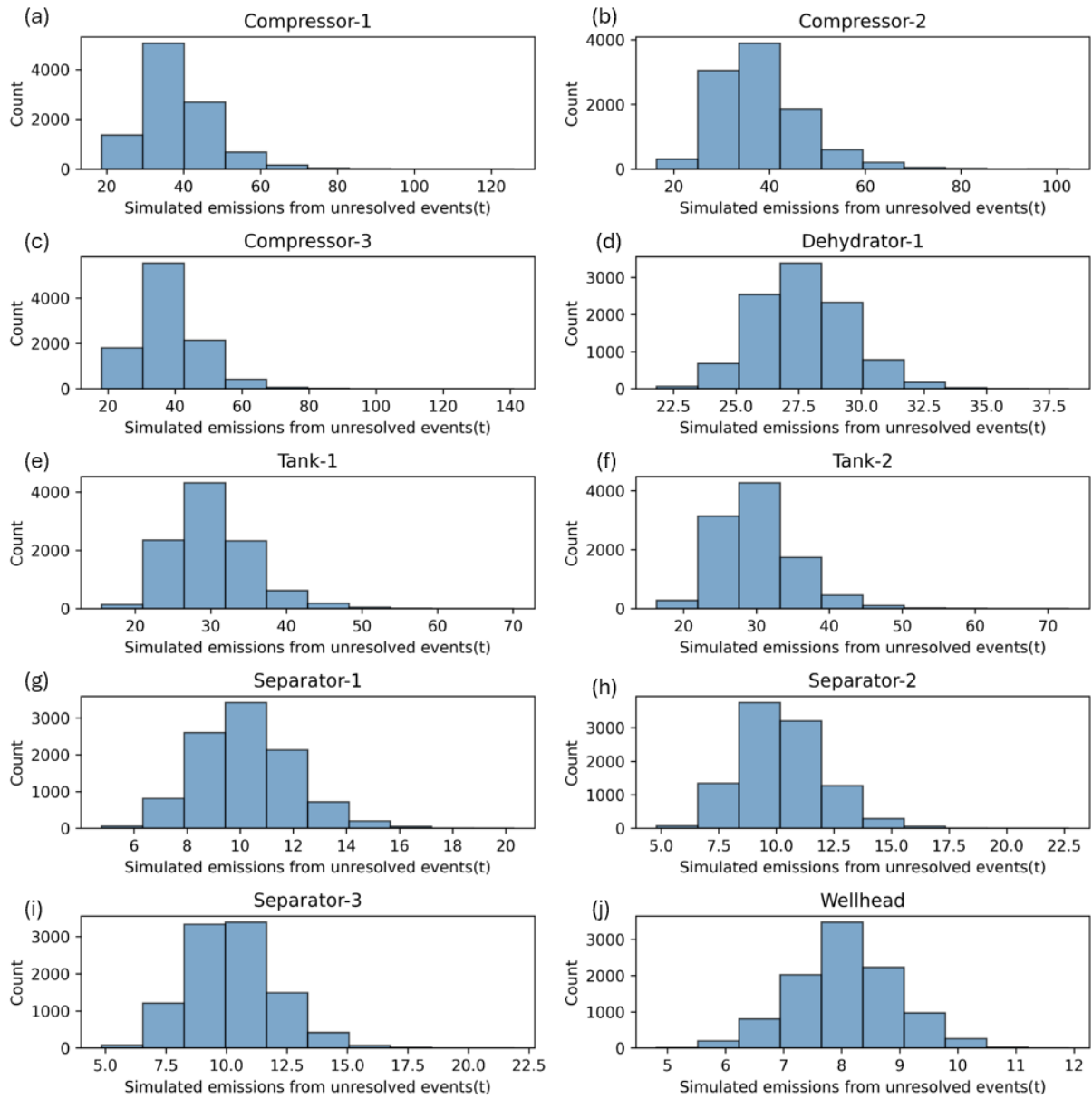


Figure S6. Unmeasured emissions distributions from after 10000 iterations of Monte Carlo runs. Plotted by fictitious equipment.

References

Allen, J.F. (1983). Maintaining knowledge about temporal intervals. *Communications of the ACM*, [online] 26(11), pp.832–843. doi:<https://doi.org/10.1145/182.358434>.

Rutherford, J.S., Sherwin, E.D., Ravikumar, A.P., Heath, G.A., Englander, J., Cooley, D., Lyon, D., Omara, M., Langfitt, Q. and Brandt, A.R. (2021). Closing the methane gap in US oil and natural gas production emissions inventories. *Nature Communications*, 12(1). doi:<https://doi.org/10.1038/s41467-021-25017-4>.